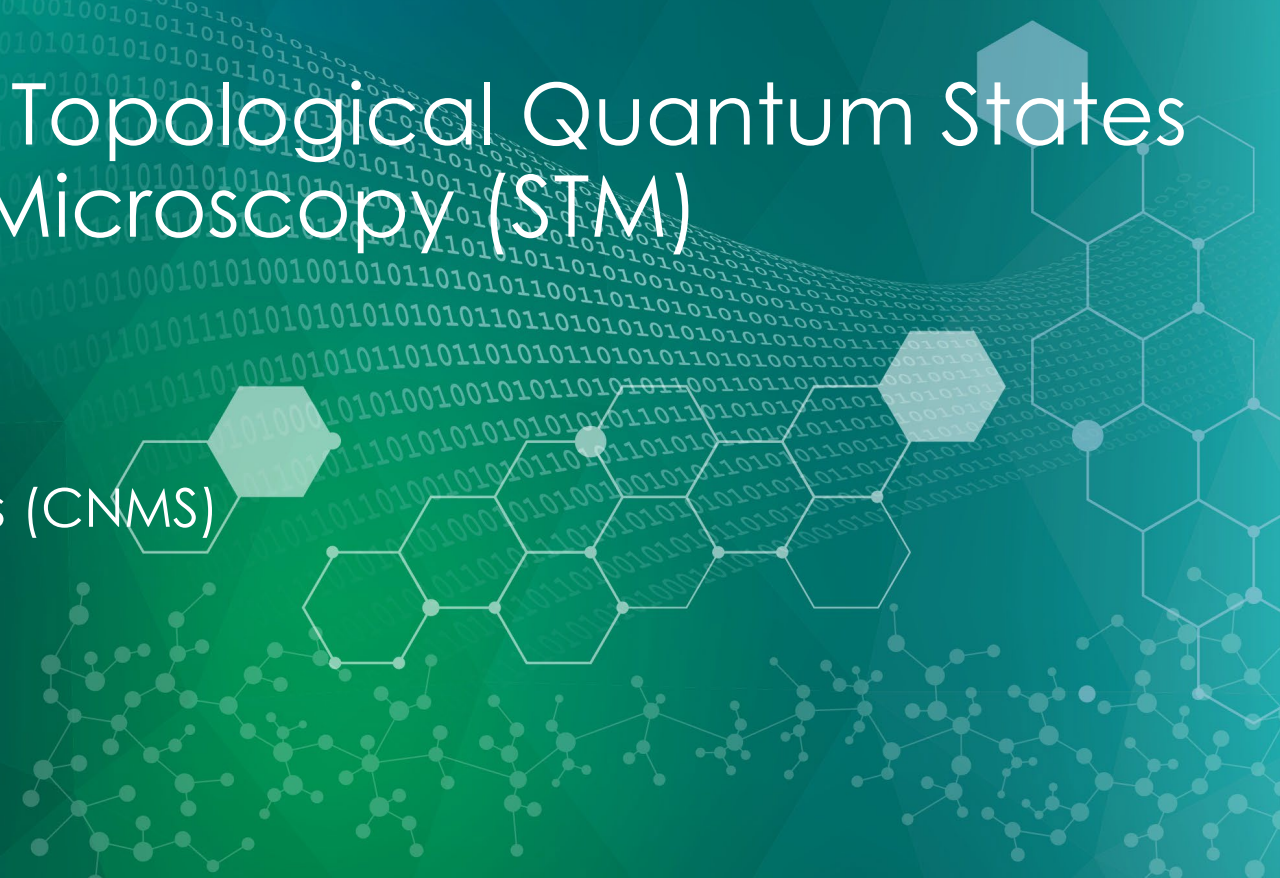


Revealing Magnetic and Topological Quantum States with Scanning Tunneling Microscopy (STM)

An-Ping Li
Center for Nanophase Materials Sciences (CNMS)
Oak Ridge National Laboratory (ORNL)

US QIS Summer School
July 15-26, 2024, ORNL, Oak Ridge, TN

ORNL is managed by UT-Battelle, LLC for the US Department of Energy



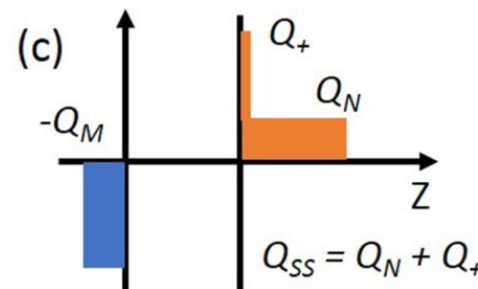
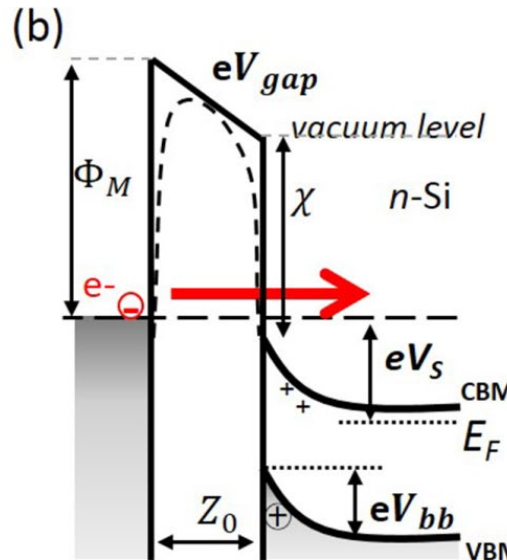
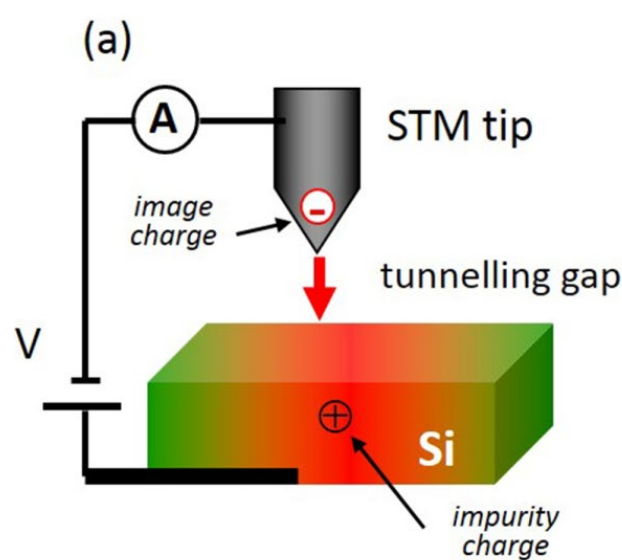
Outline

- Introductions on STM technique and the STM group in ORNL
- Image and manipulate magnetic skyrmion bubbles in a van der Waals ferromagnet Fe_3GeTe_2 using SP-STM
- Detect spin-momentum locked conductance through topological surface states on $\text{Bi}_2\text{Te}_2\text{Se}$ using SP-4-Probe STM

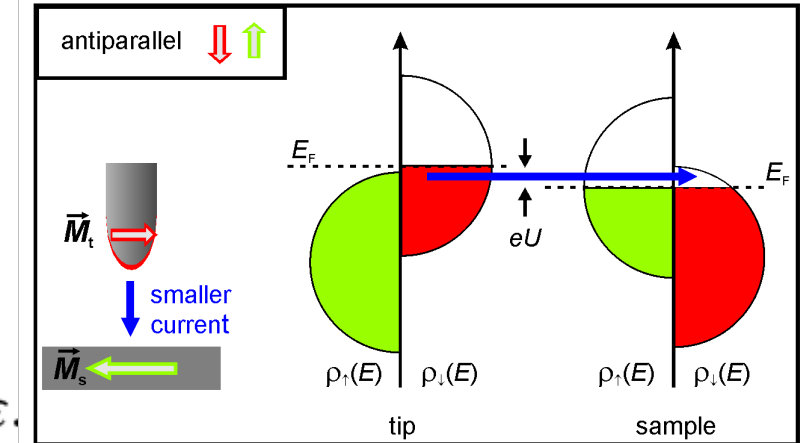
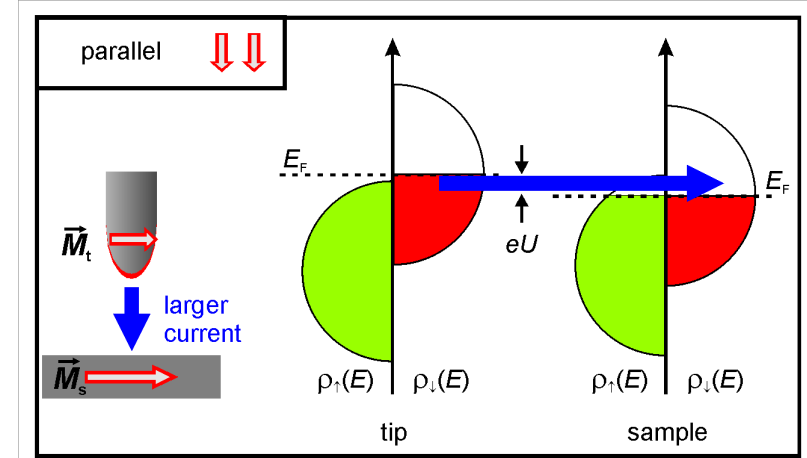
Outline

- Introductions on STM technique and the STM group in ORNL
- Image and manipulate magnetic skyrmion bubbles in a van der Waals ferromagnet Fe_3GeTe_2 using SP-STM
- Detect spin-momentum locked conductance through topological surface states on $\text{Bi}_2\text{Te}_2\text{Se}$ using SP-4-Probe STM

Electronic tunneling spectroscopy



$$I_t = \frac{4\pi e}{\hbar} \int_0^{eV} \rho_S(E_F - eV + \varepsilon) \rho_T(E_F + \varepsilon) |M|^2 d\varepsilon.$$

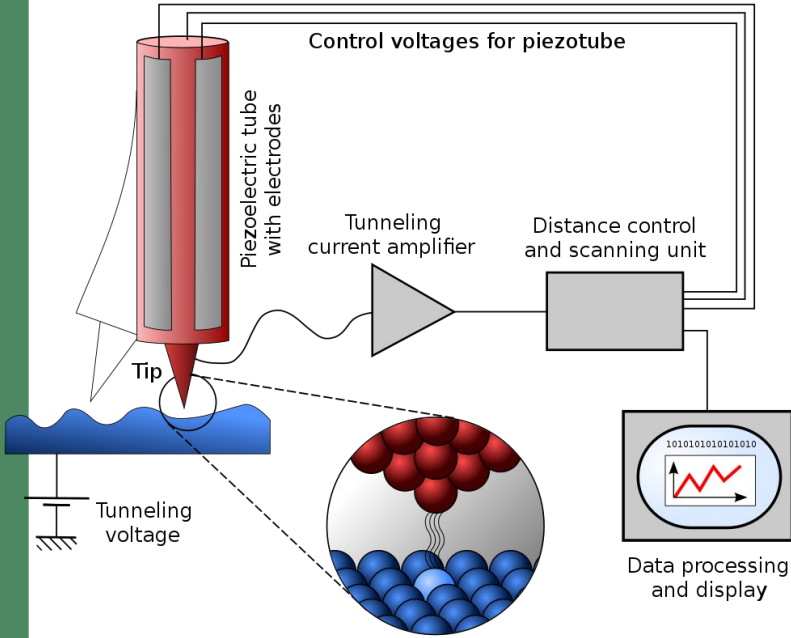


Scanning Tunneling Microscopy (STM)

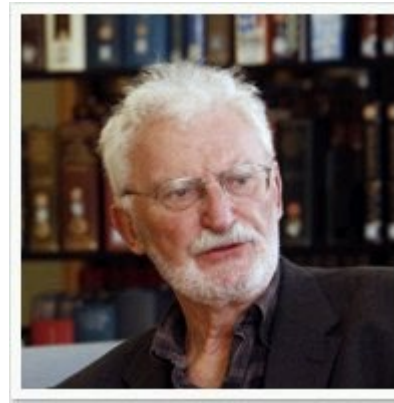
Developed in 1981



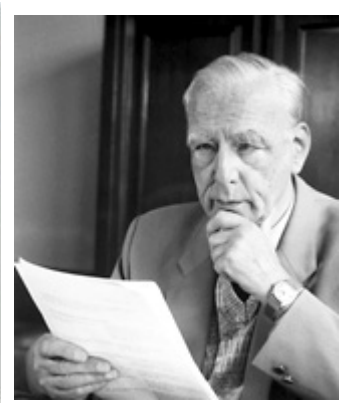
Nobel Prize in Physics 1986 for STM and electron microscopy



Gerd Binnig



Heinrich Rohrer



Ernst Ruska

STM

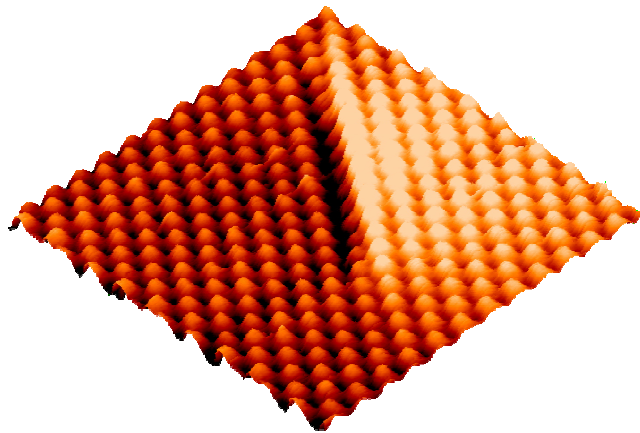
EM

STM is the instrument for imaging surfaces at the atomic level

History of STM at ORNL and STM Group Science

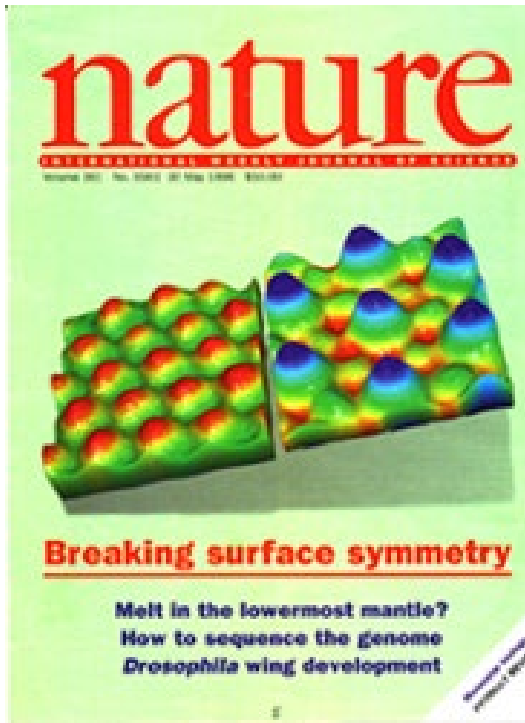
STM History at ORNL:

Topography



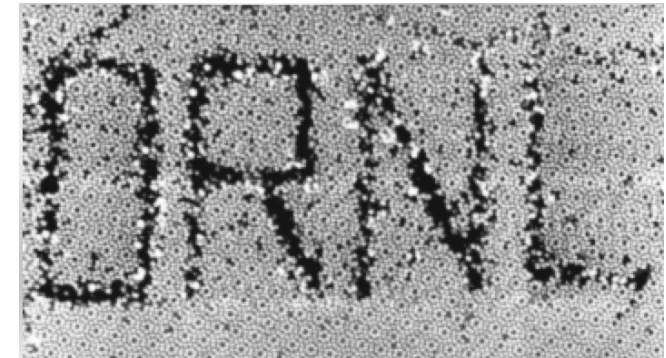
Dislocation, J. Wendelken, ORNL, 1995

Electronic density of states



Charge density wave,
W. Plummer, ORNL, 1996

Manipulation

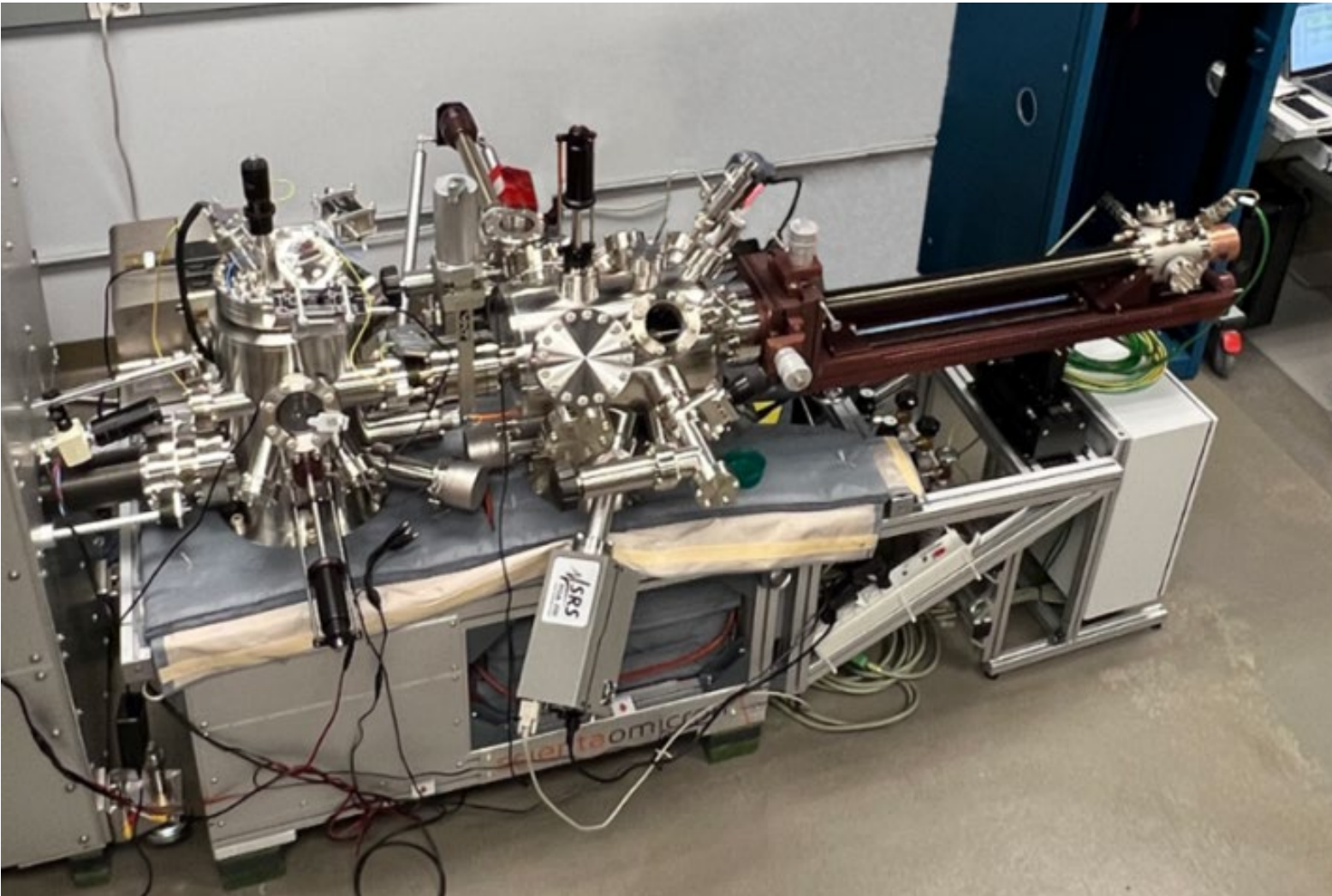


Atom manipulation,
W. Plummer, ORNL, 1995

STM Group Science:

Observing, characterizing, and manipulating atoms and nanostructures on materials to elucidate complex correlations of the atomic constituents and their fundamental electronic properties

A typical STM



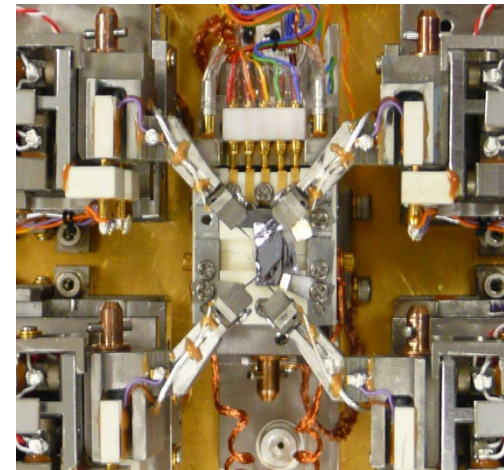
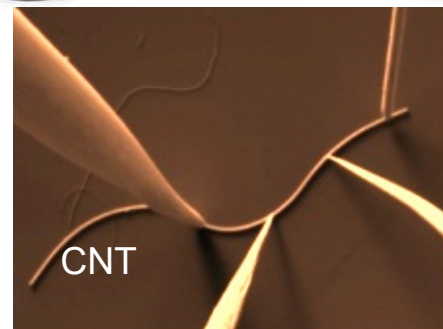
Features of ORNL Infinity LT-STM

- STM/STS from 10-300 K with atomic resolution
- q-Plus AFM
- Nanonis control system with CNMS developed control and analysis tools
- High temperature tip cleaning
- Ar ion sample sputtering annealing to 800 K
- MBE deposition sources
- Controlled gas exposures
- Low Energy Electron Diffraction (LEED)



Cryogenic Four-Probe STM

ORNL 4-Probe STM
Installed in 2006

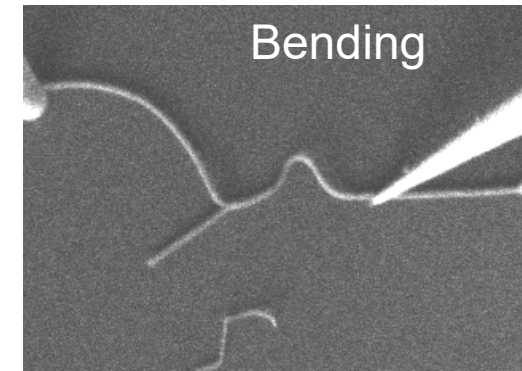
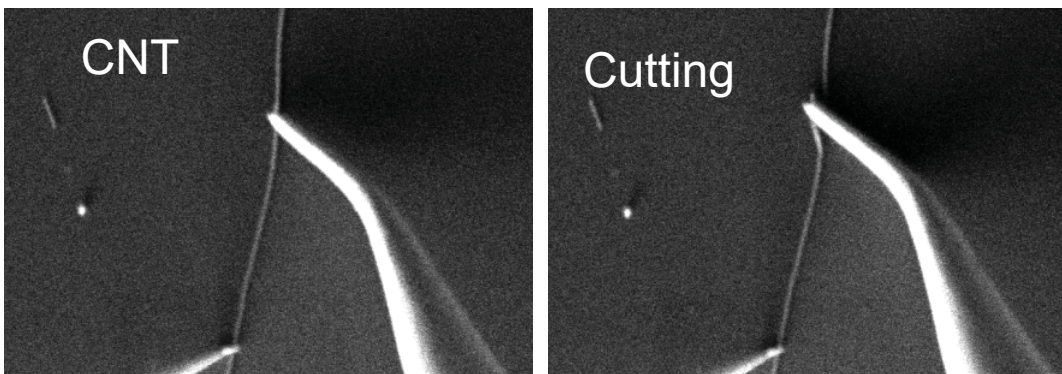
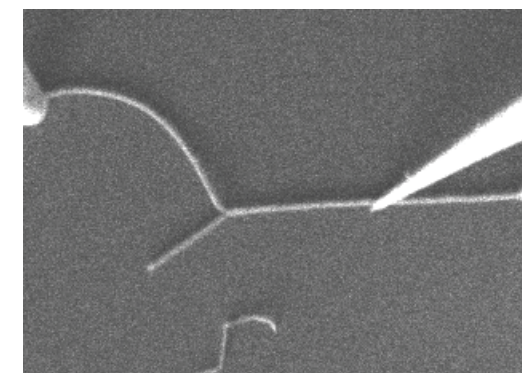
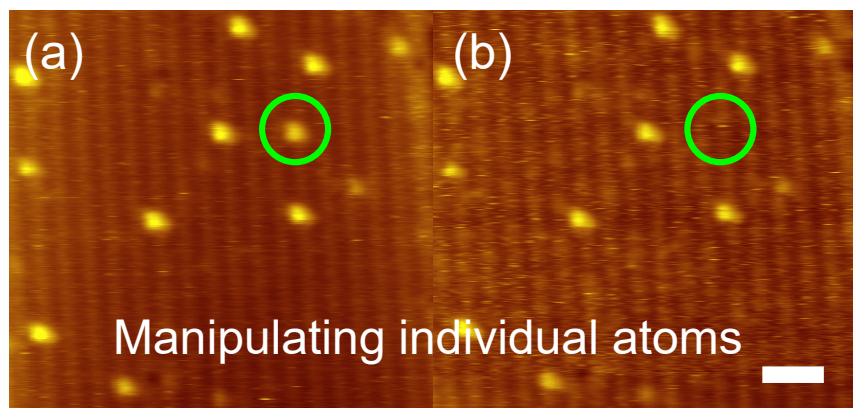
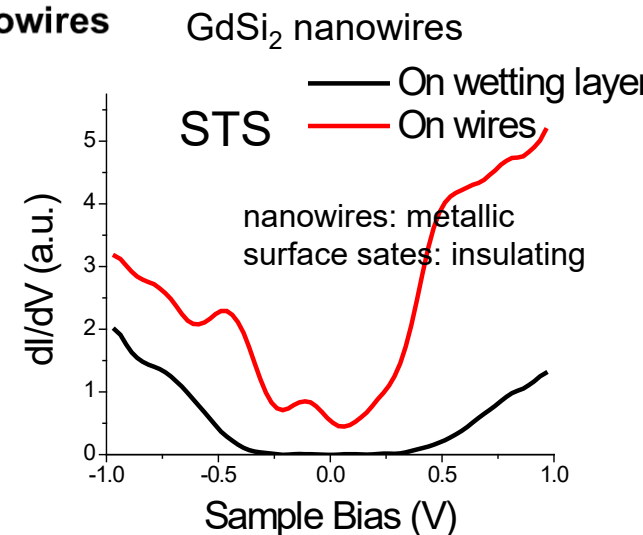
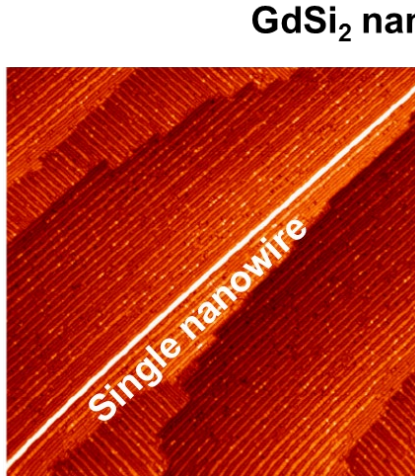
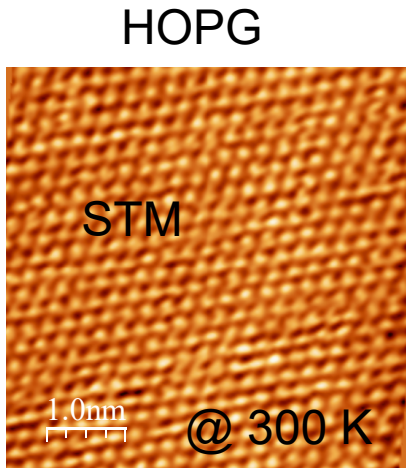


Unisoku/RHK QuadraProbe STM

- Cryogenic (10-300 K)
- Atomic resolution imaging, spectroscopy
- Nanoscale transport
- Nanomanipulation and nanofabrication
- SEM/MBE/SAM
- Tuning fork-AFM/STM

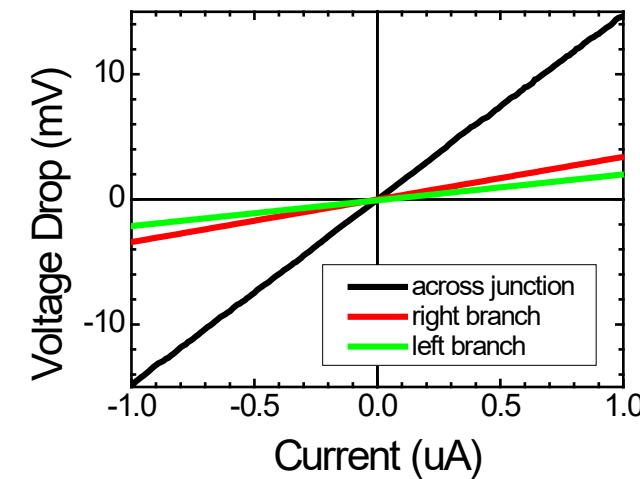
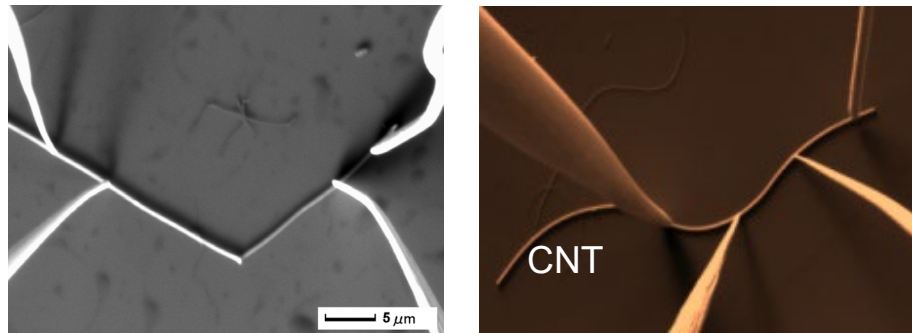
Kim et al., Rev. Sci. Instrum. 78, 12370 (2007)

Imaging, spectroscopy, and manipulation

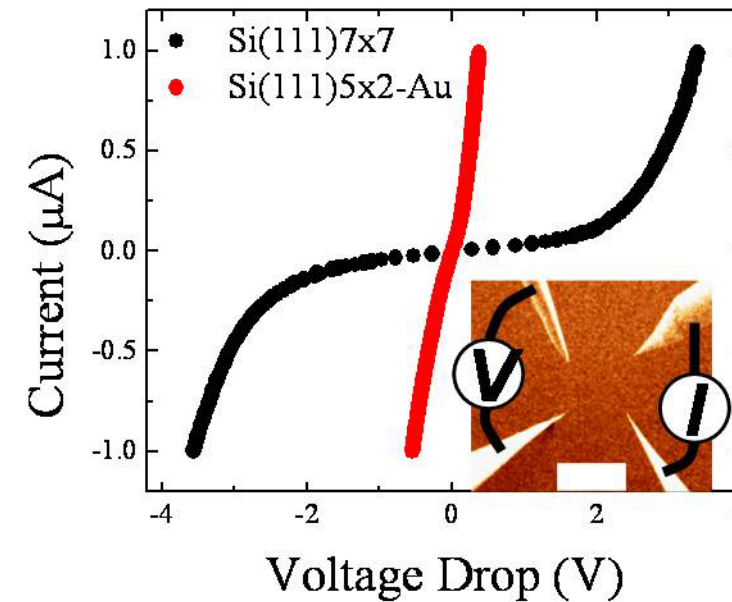
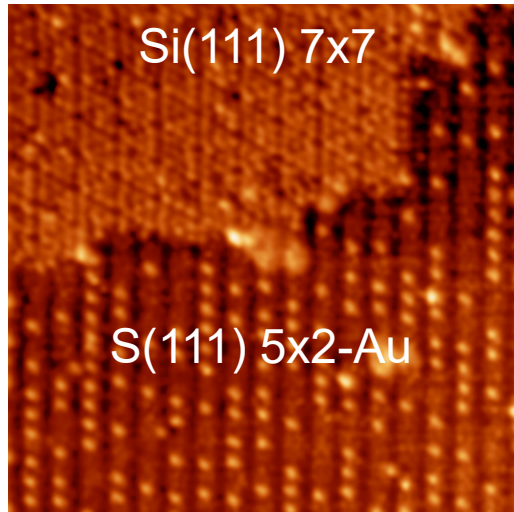


Electrical transport for nanomaterials

Transport in 1D



Transport in 2D



A suite of STM at CNMS of ORNL for atomic-scale imaging, spectroscopy, and manipulation

Single-probe STM



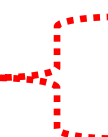
- Omicron-VT (30 – 600K) STM/AFM + MBE (metal and semiconductors) – [J-G43 \(8610\)](#)
- Home-built cryogenic STM + MBE (organic molecules) – [J-G43 \(8610\)](#)
- Home-built HB (9T) LT (2K) STM (superconductors) – [J-G43 \(8610\)](#)
- Omicron VT STM/AFM + PLD (oxides) – [J-G47 \(8610\)](#)
- Unisoku 40mK vector field (9-2-2T) STM (spin detection) – [L120 \(4515\)](#)
- Omicron Infinity Close-Cycle LT (10 – 420 K) STM (atom/molecule manipulations) – [L120 \(4515\)](#)
- SPECS Joule-Thomson STM/AFM (1.2 – 300 K) (Josephson tunneling/molecules) – [112 \(3516\)](#)

Four-probe STM



- Customized RHK/Unisoku LT (10K) 4-probe STM (transport) – [J-G47 \(8610\)](#)
- Omicron LT (4.5K) 4-probe STM/AFM (atomic imaging, transport, manipulation) – [L121 \(4515\)](#)

Magneto-meter



- SQUID Magnetometer – Magnetic Property Measurement System – [J-155 \(8610\)](#)
- Scanning NV Magnetometer – [C141\(4100\)](#)

Materials of interest

Nanostructured Materials

- Heterogeneities in atomic lattices
 - Defect structures and their multiple degrees of freedom (electronic, magnetic, ..)
 - Structure-property relationship
- Controlled positioning and manipulation of individual dopants/defects
- Confined boundary states
 - Interaction of 2D vdw layers
 - Interfacial states

Published Reviews on Topic:

Adv. Func. Mater. **29**, 1903770(2019);
Prog. Surf. Sci. **92**, 176(2017)

Quantum Materials

- Quasiparticle states in topological matter
 - Topological surface/edge states
 - Magnetic skyrmions
 - Majorana bound states
- Dissipationless edge current
 - Spin-momentum locked current
 - Quantum anomalous Hall effect
- Superconductivity
 - Competing order parameters in superconductors
 - Topological superconductivity

Adv. Mater. **35**, 2106909 (2023)

Molecular Materials

- On-surface synthesis of graphene nanoribbons with atomic precision
 - Long GNR arrays
 - In situ assessment of intrinsic electronic, magnetic, and transport properties
- Atomic precise molecular heterostructures for single photon emission
 - Large quantity of “identical” heterojunctions
 - Correlation of atomic/electronic structures with optical behaviors
- Directed molecular motions and reactions

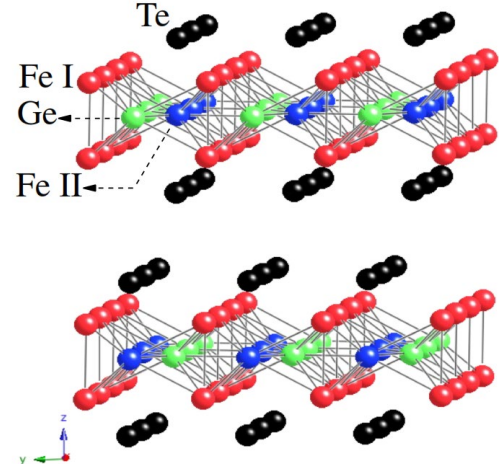
Nat. Rev. Phys. **3**, 791 (2021)

Outline

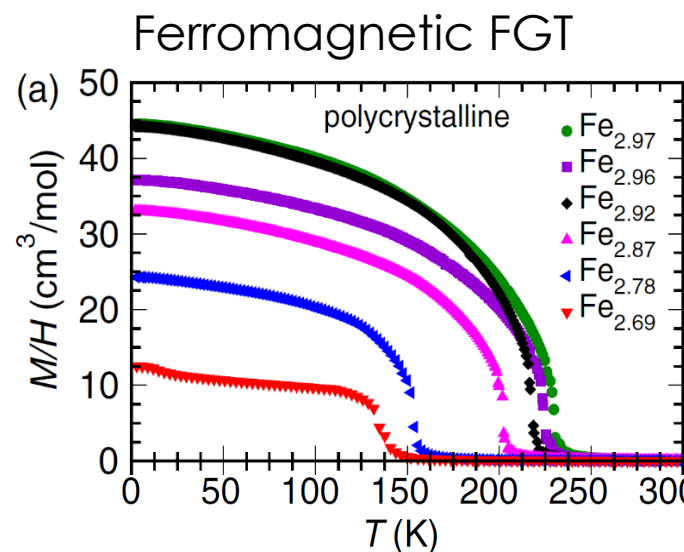
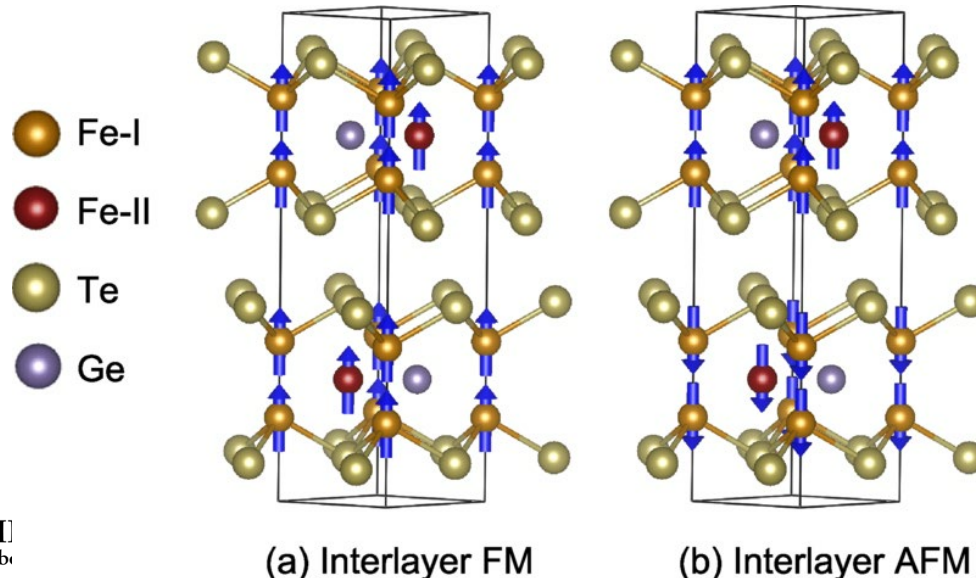
- Introductions on STM technique and the STM group in ORNL
- Image and manipulate magnetic skyrmion bubbles in a van der Waals ferromagnet Fe_3GeTe_2 using SP-STM
- Detect spin-momentum locked conductance through topological surface states on $\text{Bi}_2\text{Te}_2\text{Se}$ using SP-4-Probe STM

Image and manipulate magnetic skyrmion bubbles in a van der Waals ferromagnet Fe_3GeTe_2

Crystal structure



B. Chen et al., J. Phys. Soc. Jpn (2013)



High bulk magnetic transition temperature
 $T_c > 200\text{K}$

A. F. May et al, PRB **93**, 014411 (2016).

Ferromagnetic interlayer coupling:

H.-J. Deiseroth et al, Eur. J. Inorg. Chem. **2006**, 1561 (2006).

B. Chen et al, J. Phys. Soc. Jpn. **82**, 124711 (2013).

V. Y. Verchenko et al, Inorg. Chem. **54**, 8598 (2015).

N. León-Brito et al, J. Appl. Phys. **120**, 083903 (2016).

A. F. May et al, Phys. Rev. B **93**, 014411 (2016).

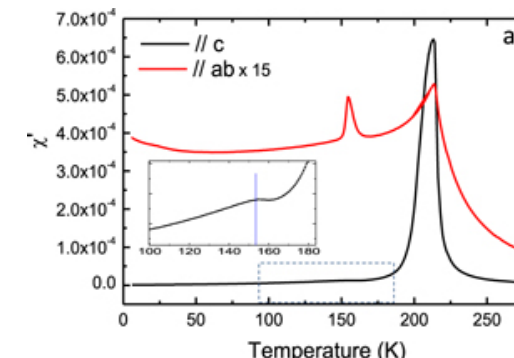
J.-X. Zhu et al, Phys. Rev. B **93**, 144404 (2016).

H. L. Zhuang et al, Phys. Rev. B **93**, 134407 (2016).

Y. Liu et al., Phys. Rev. B **96**, 144429 (2017).

Antiferromagnetic interlayer coupling:

J. Yi et al, 2D Mater. **4**, 011005 (2016).

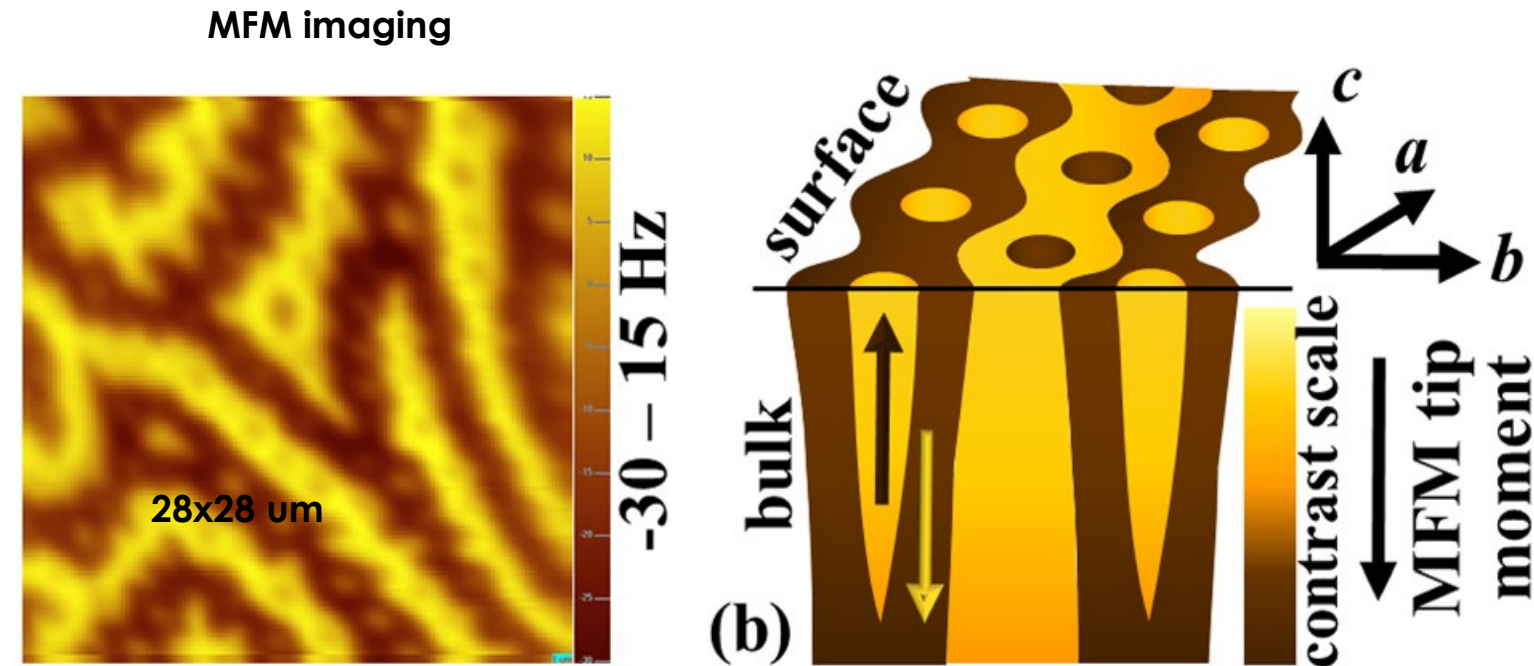
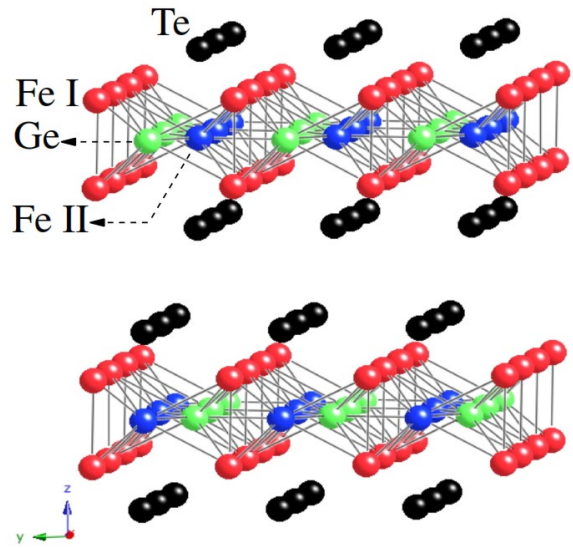


- What is the nature of interlayer coupling?

Magnetic domains in a van der Waals ferromagnet Fe_3GeTe_2

Magnetic ordering temperature ($140\text{K} < T_c < 230\text{K}$) and magnetic anisotropy are reduced with increasing concentration of Fe-II vacancies

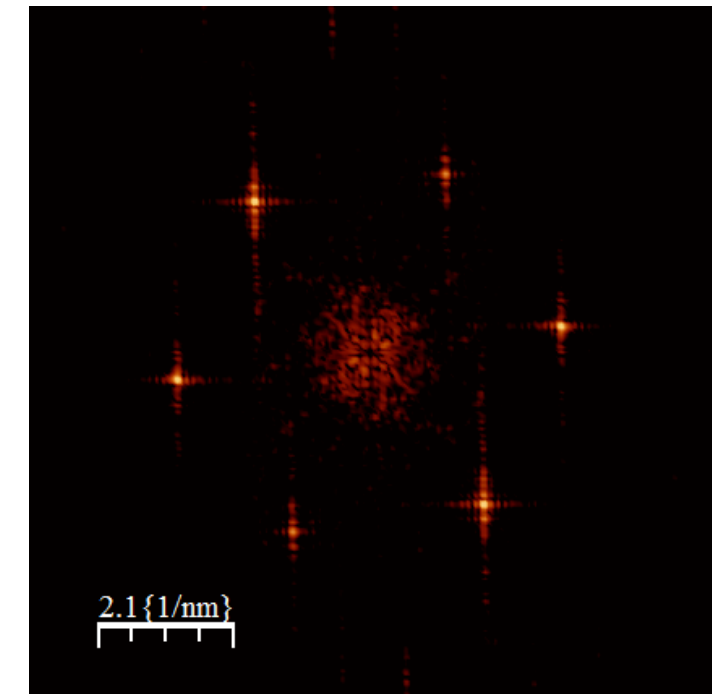
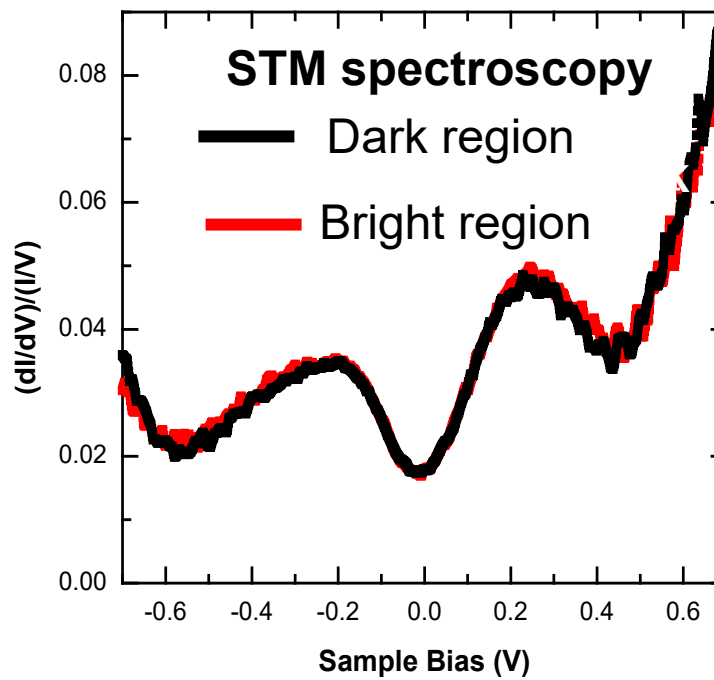
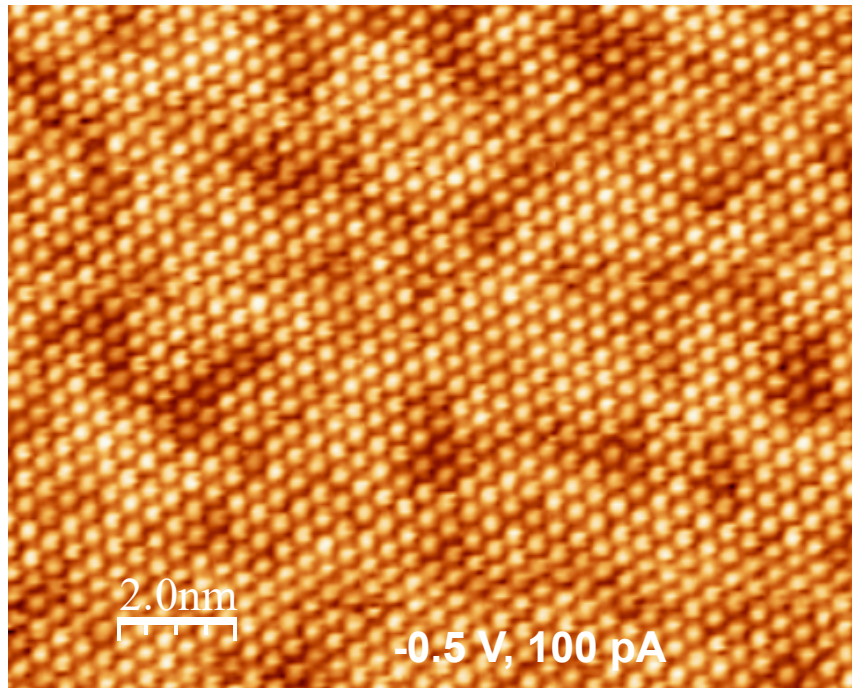
A. F. May et al, [PRB 93, 014411 \(2016\)](#).



N. Leon-Brito et al., J. Appl. Phys. 120, 083903(2016)

- **What is the nature of magnetic domains?**
- **What role does the Fe-II vacancy play?**

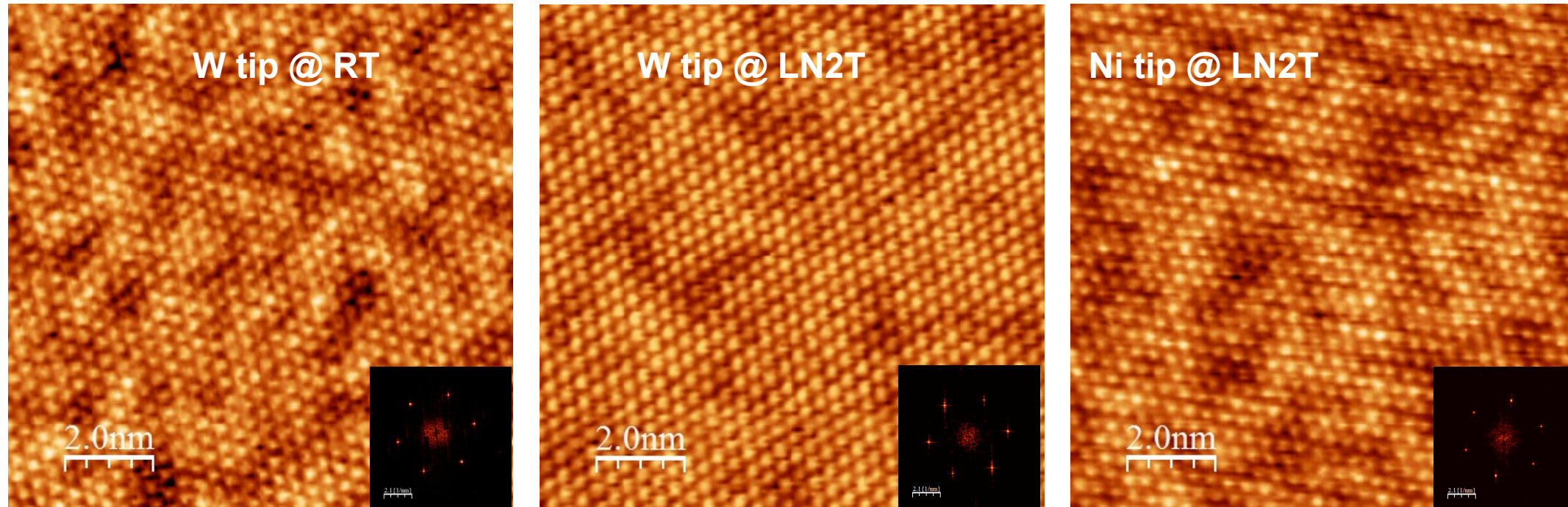
STM image of Fe_3GeTe_2



Atomic domain: depressed atoms
Depressed height: 13 to 50 pm
Area density: $23 \pm 4\%$

Atomic scale domains without long range order

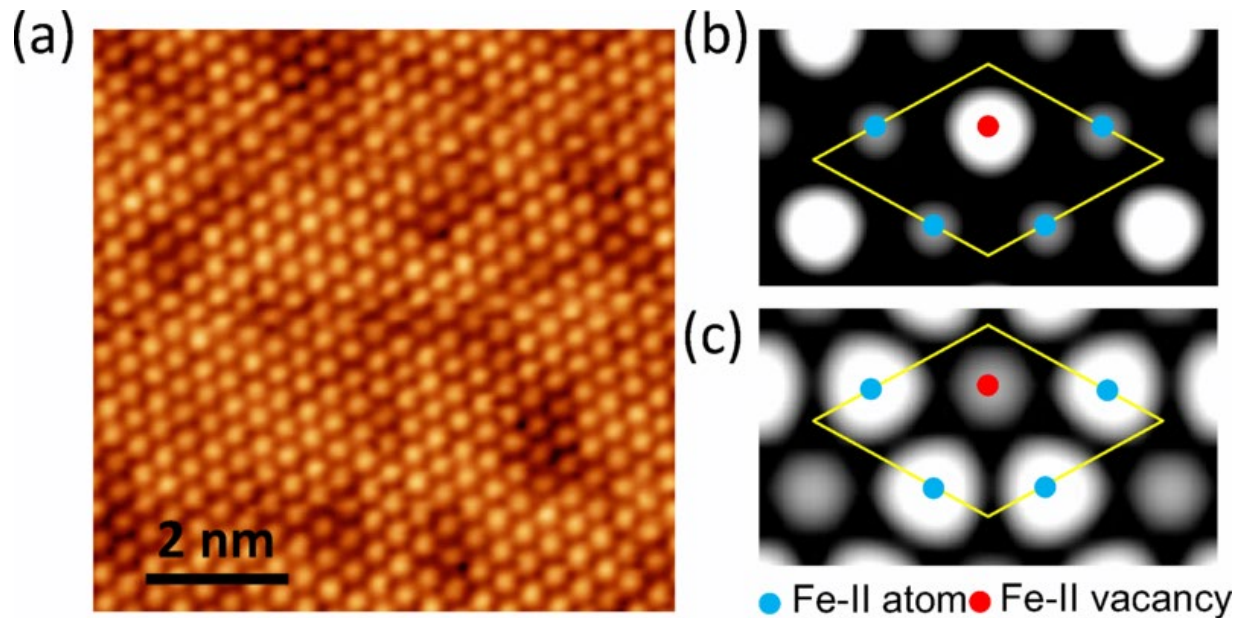
SP-STM at the atomic scale



No magnetic contrast at the atomic scale

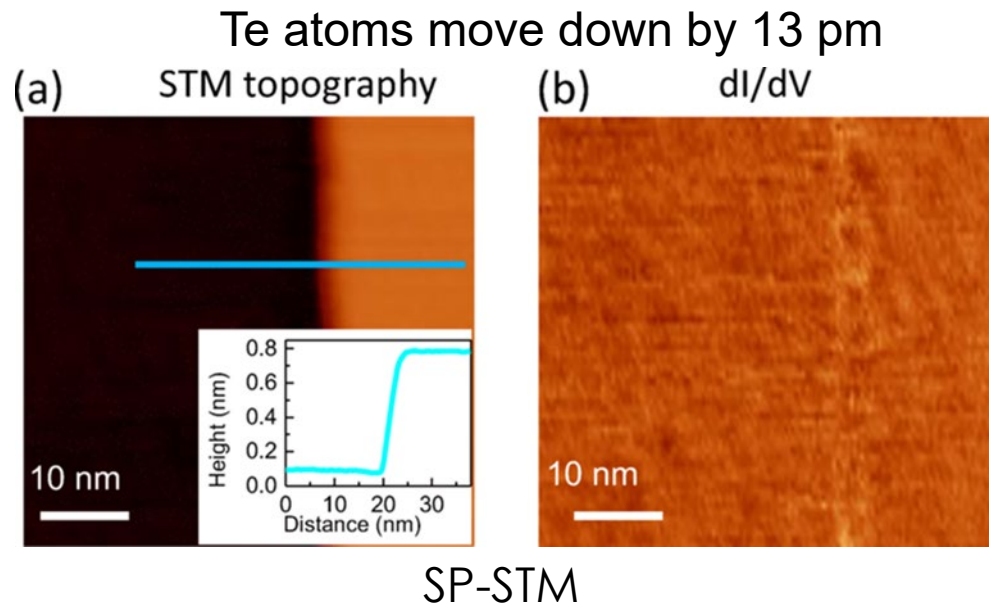
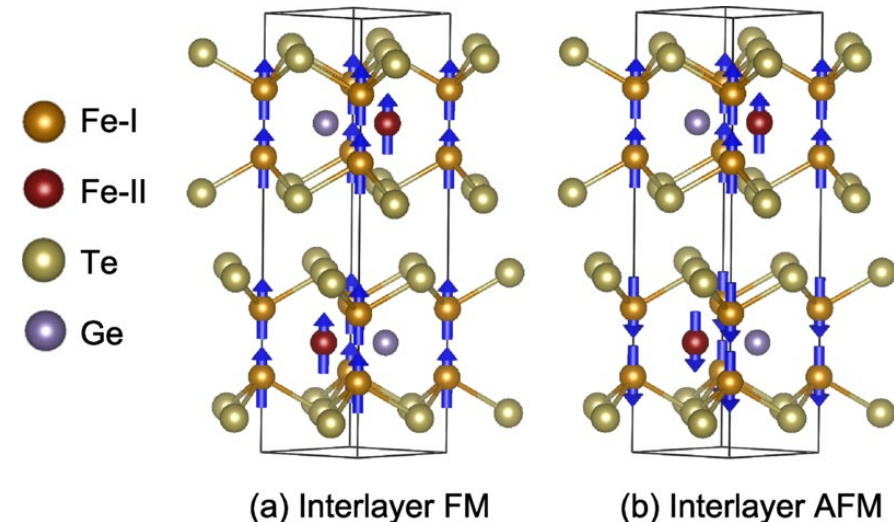
Atomic domains are not the magnetic domains observed at a larger length scale

Interlayer coupling of Fe₃GeTe₂



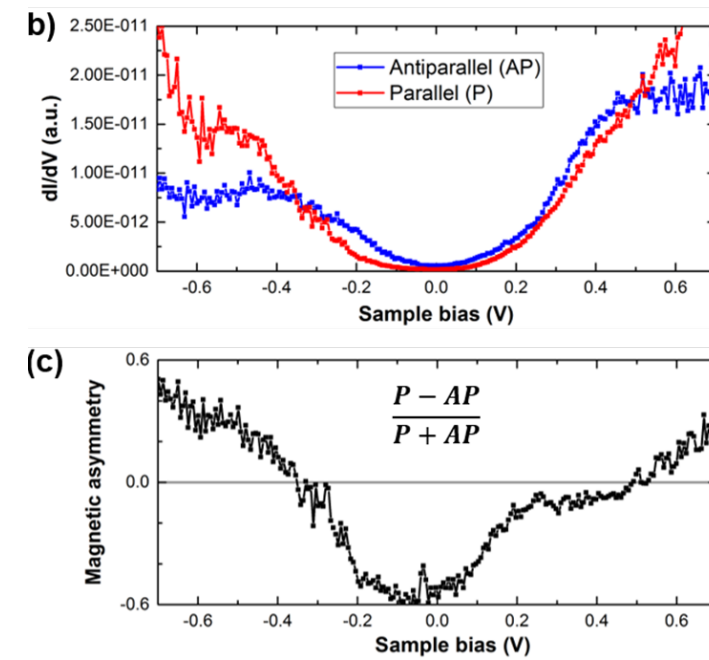
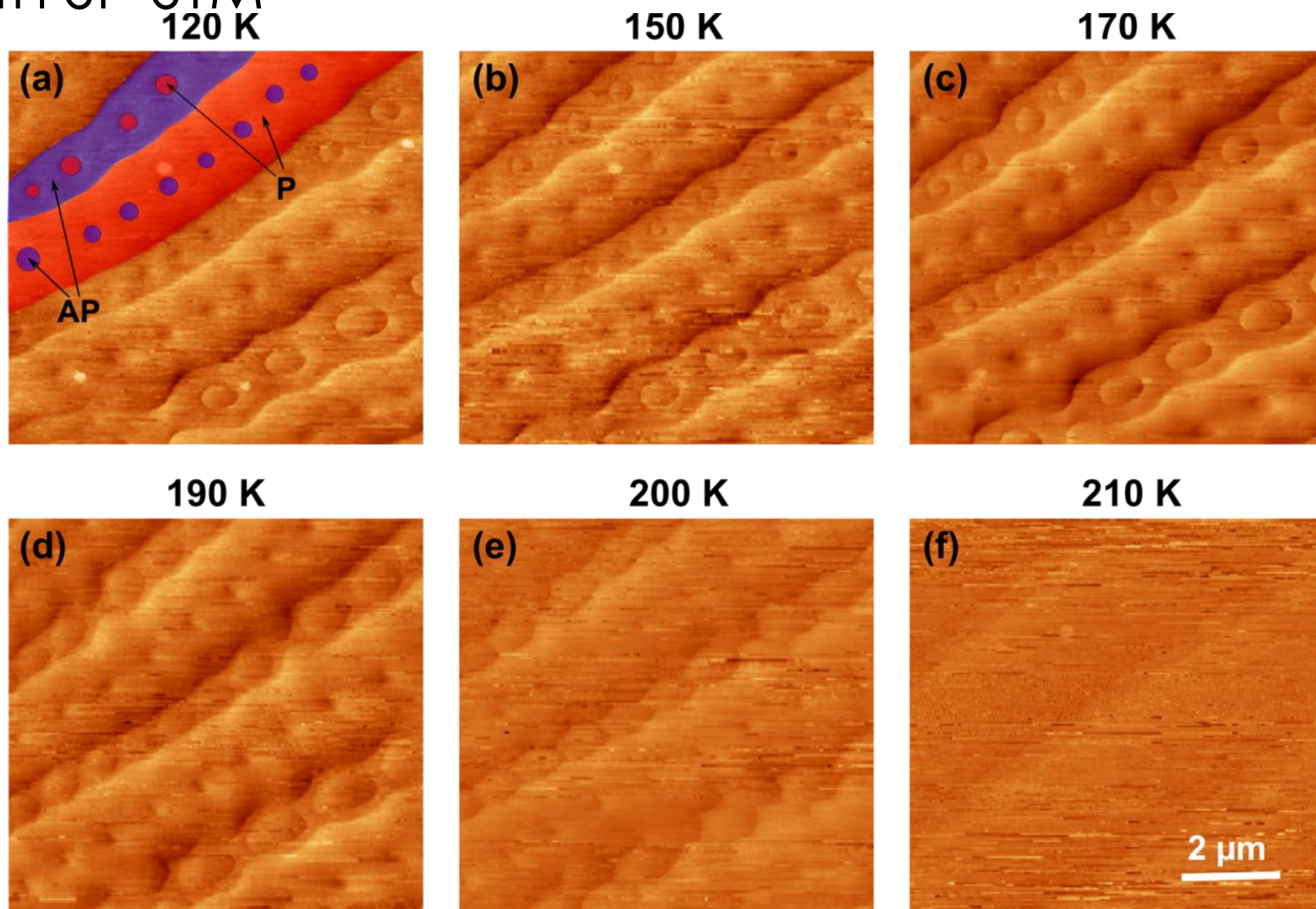
X. Kong et al, Phys. Rev. Materials **4**, 094403 (2020)

Atomic domains come from Fe-II vacancies which show inhomogeneous distributions



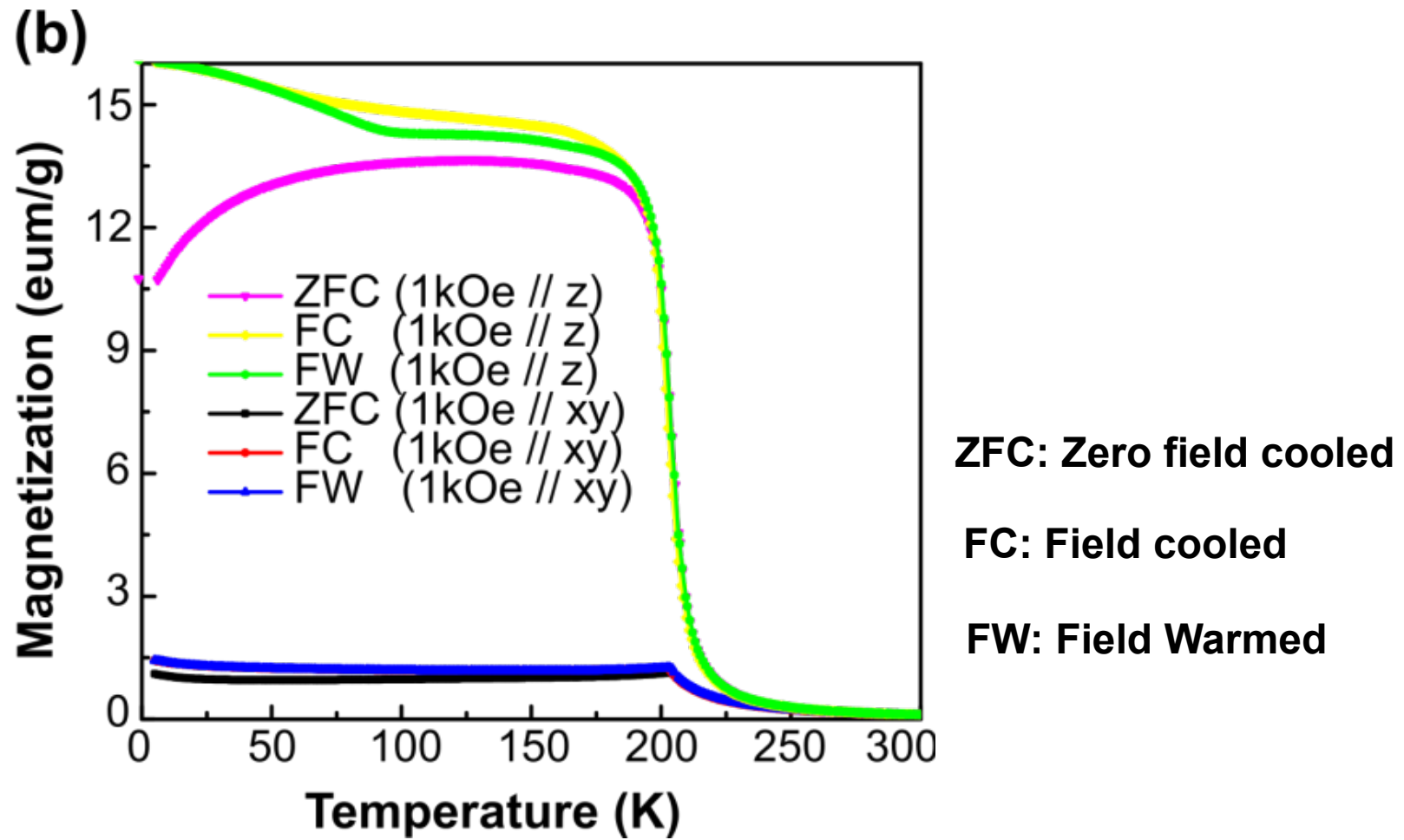
Layers of FGT are coupled ferromagnetically

Temperature dependence of ZFC magnetic domains revealed with SP-STM

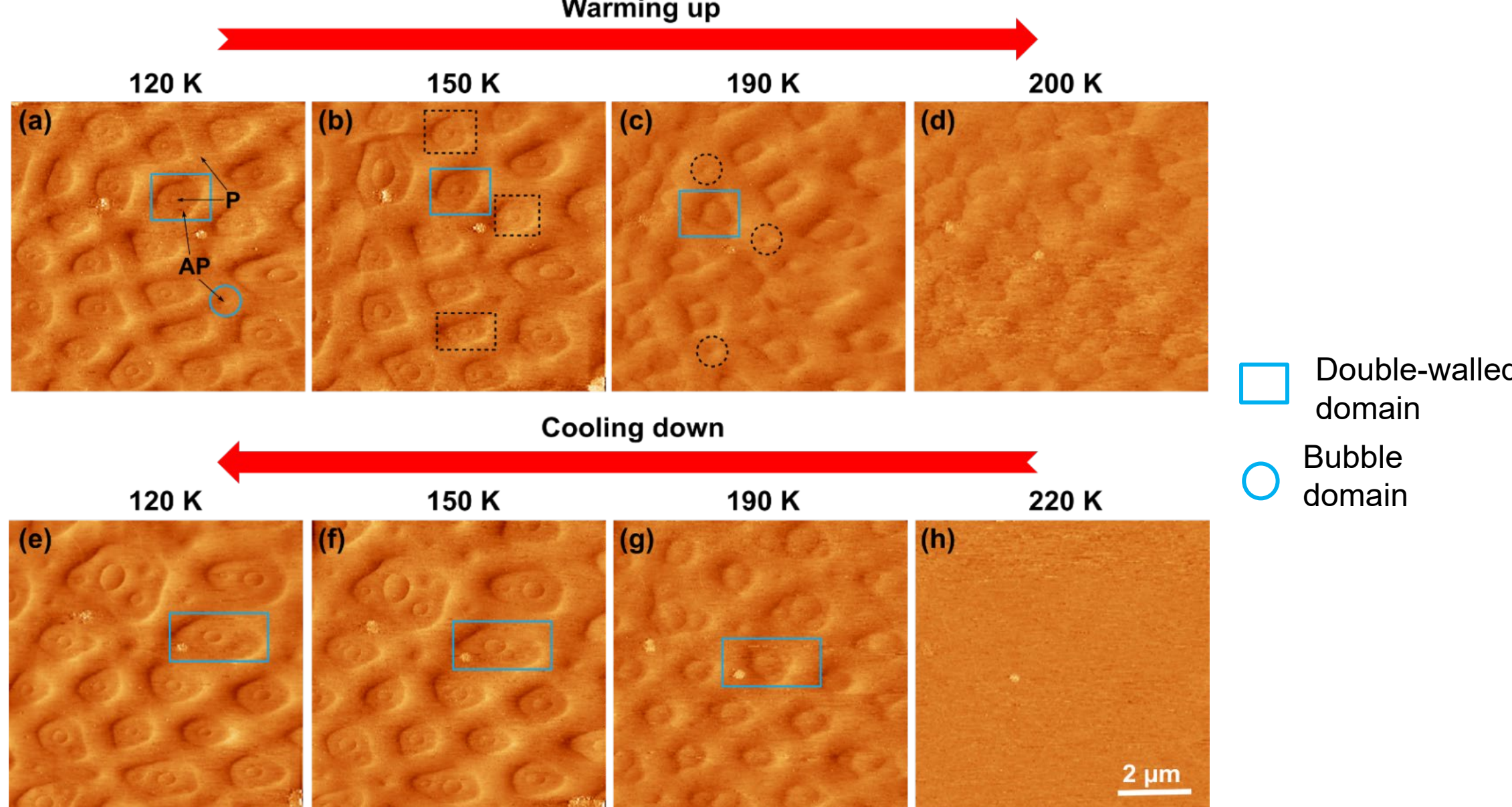


✓ Transition temperature: 200-210 K

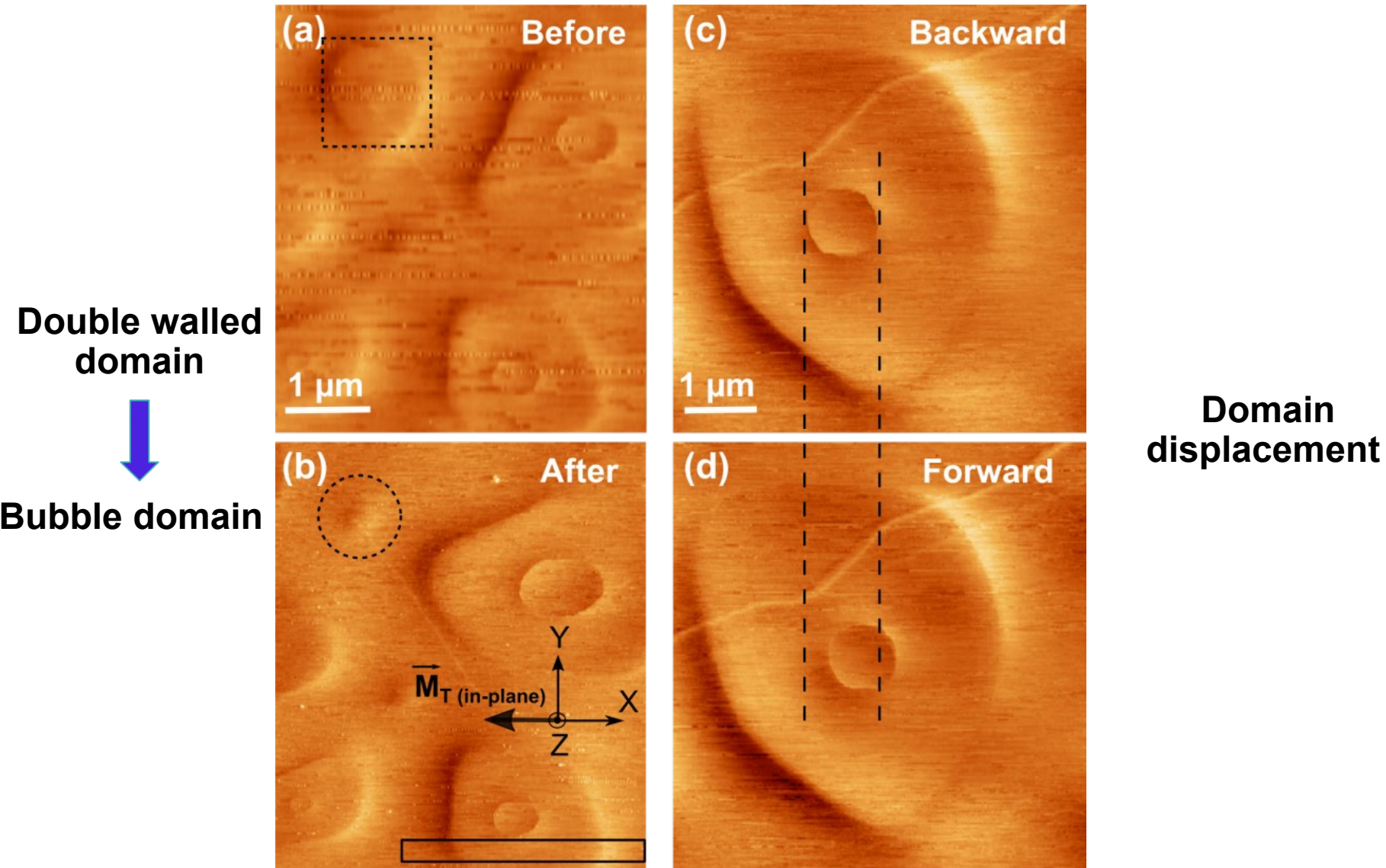
SQUID measurement



Temperature dependence of FC domains

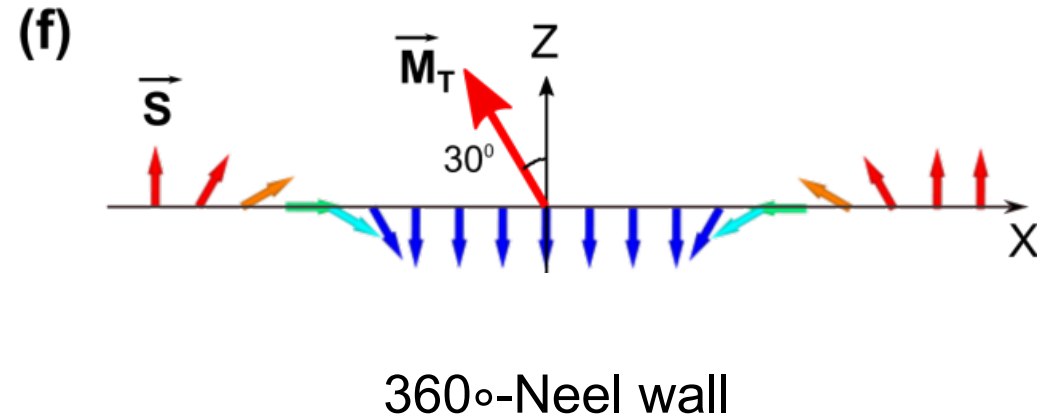
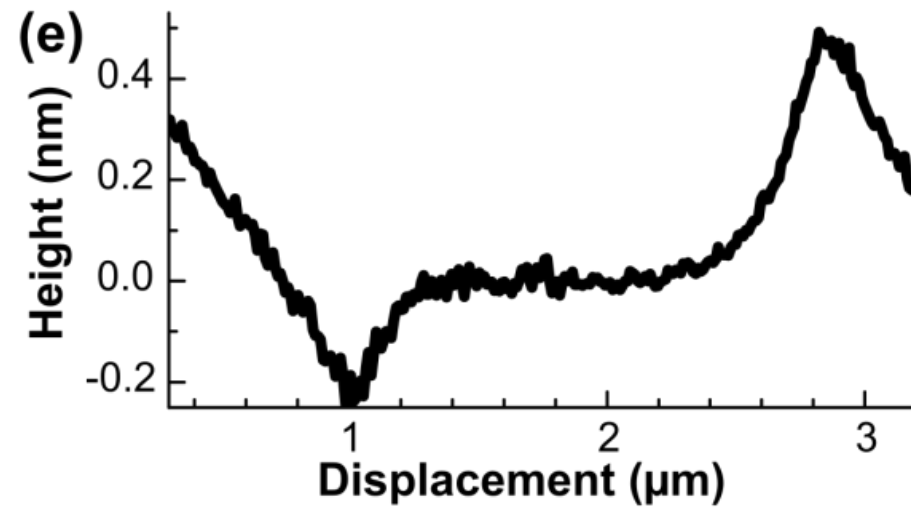
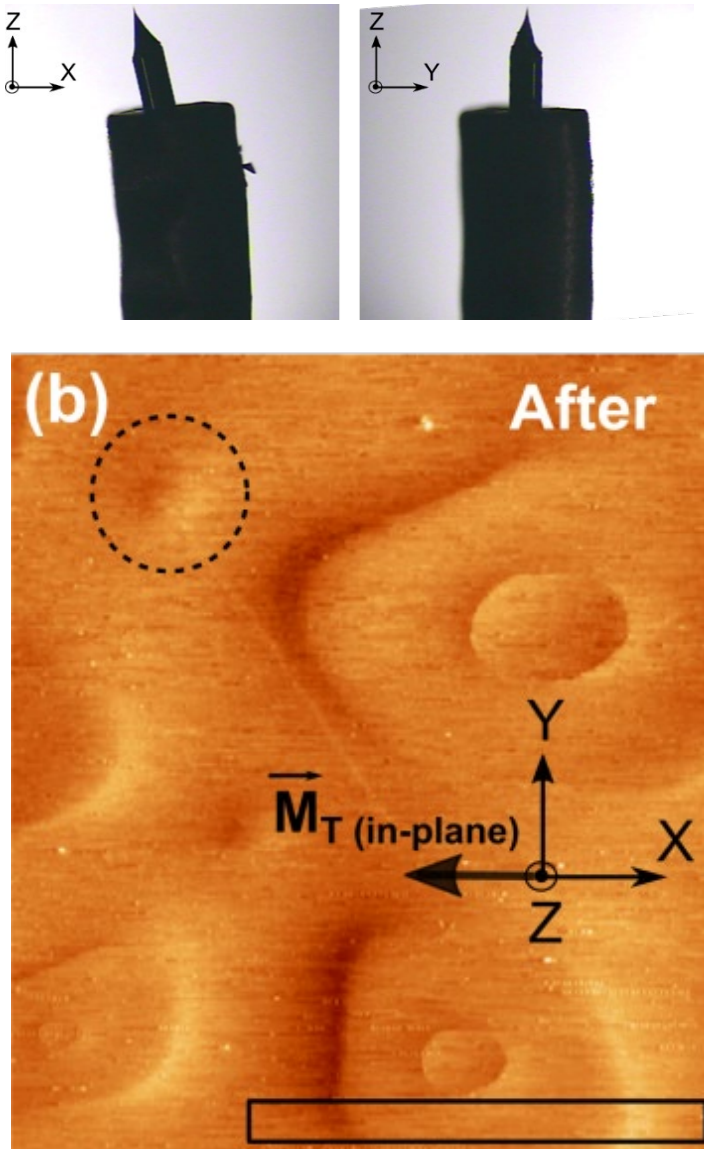


Tip manipulation of FC domain

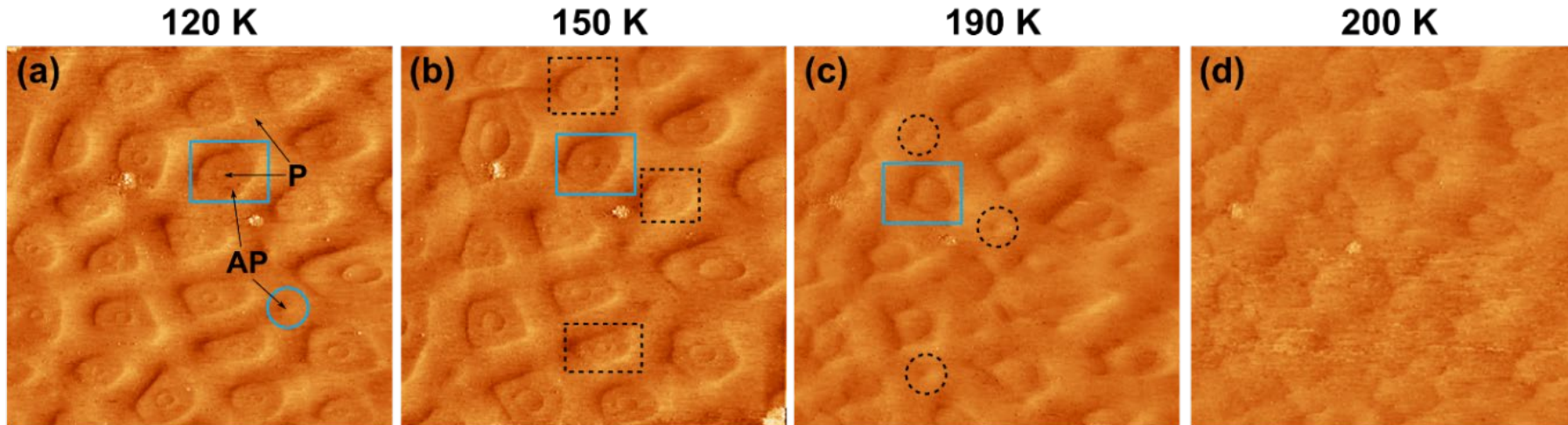


Neel type domain wall structure

Images of the SP-STM tip



Neel-type skyrmion observed in FGT



- Spin texture with 360° rotation across the domain.
- Emergence of the circular domain structure from stripy domain shows that a magnetic field promotes the formation of skyrmion phase from a helical phase.
- Size of the skyrmion bubble (100 nm to 1 μm) due to a competition of long-range dipolar interactions with shape anisotropy.

Mechanisms of skyrmion formation

- Dzyaloshinskii–Moriya exchange interaction (DMI) in magnets without inversion center and a weak magnetic anisotropy
 - Observed skyrmion structure in FGT, inconsistent with its presumed centrosymmetric structure
- Interfacial DMI could account for the observation of chiral Néel skyrmions in an otherwise centrosymmetric compound
 - Observed skyrmion structure in FGT, inconsistent with its presumed bulk structure
- Fe vacancies break the inversion symmetry?
- “further investigation is required to confirm if the magnetic domain structures observed here have any topologically protected nature of skyrmions”.

G.D. Nguyen et al, Physical Review B 97, 014425 (2018)

Lorentz transmission electron microscopy (LTEM)

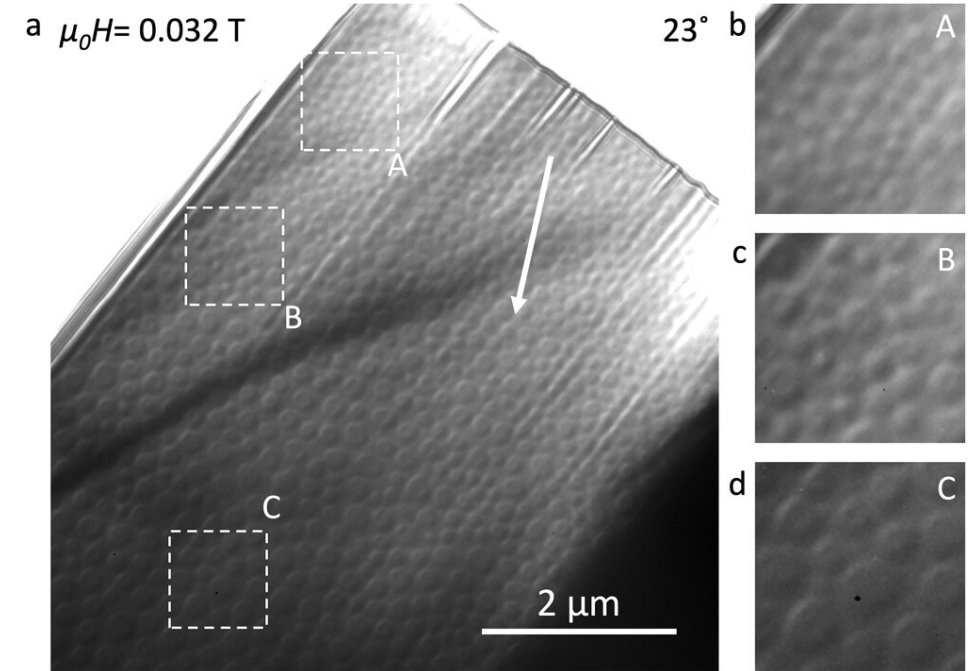
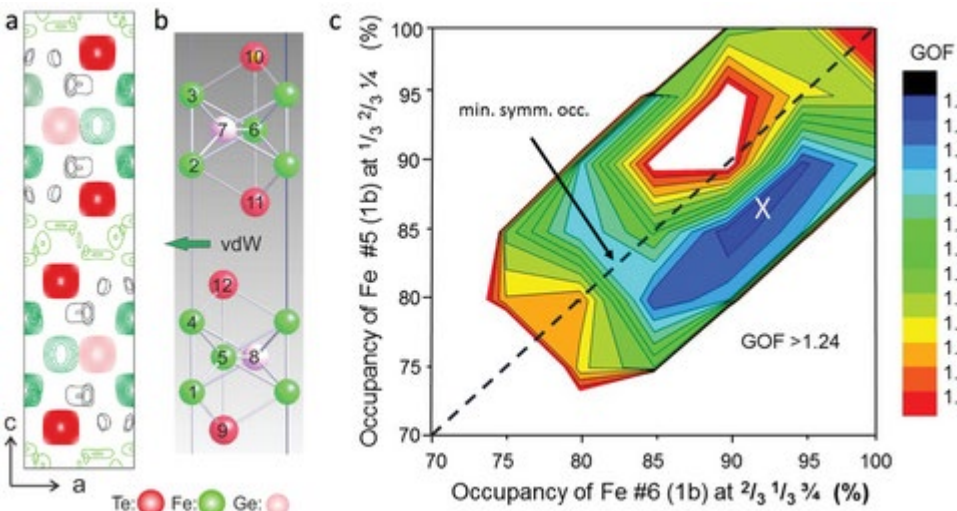
ADVANCED MATERIALS

Research Article | Open Access |

Magnetic Skyrmions in a Thickness Tunable 2D Ferromagnet from a Defect Driven Dzyaloshinskii–Moriya Interaction

Anirban Chakraborty, Abhay K. Srivastava, Ankit K. Sharma, Ajesh K. Gopi, Katayoon Mohseni, Arthur Ernst, Hakan Deniz, Binoy Krishna Hazra, Souvik Das, Paolo Sessi, Ilya Kostanovskiy, Tianping Ma, Holger L. Meyerheim, Stuart S. P. Parkin ... See fewer authors ^

First published: 19 January 2022 | <https://doi.org/10.1002/adma.202108637> | Citations: 17

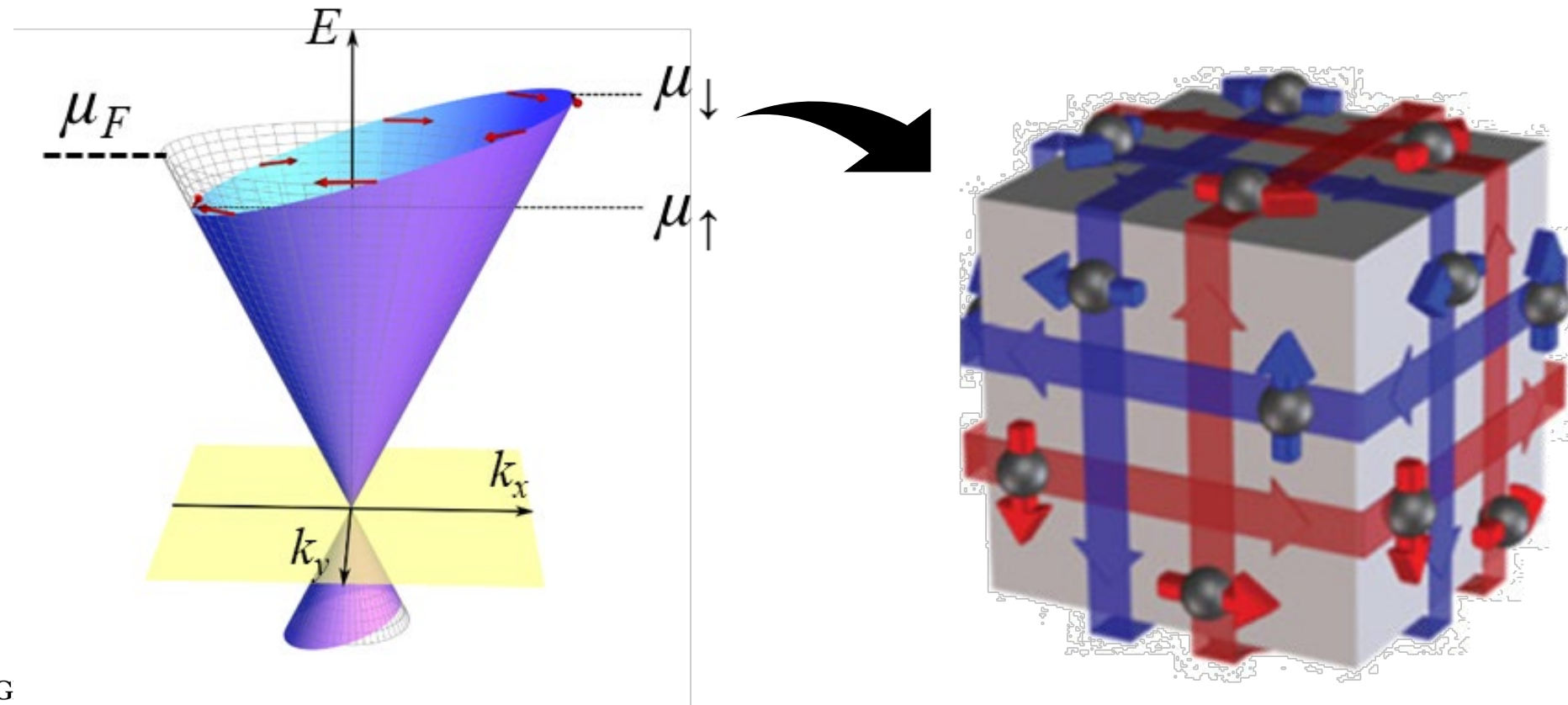


Outline

- Introductions on STM technique and the STM group in ORNL
- Image and manipulate magnetic skyrmion bubbles in a van der Waals ferromagnet Fe_3GeTe_2 using SP-STM
- Detect spin-momentum locked conductance through topological surface states on $\text{Bi}_2\text{Te}_2\text{Se}$ using SP-4-Probe STM

Spin-momentum-locked conduction in topological insulators

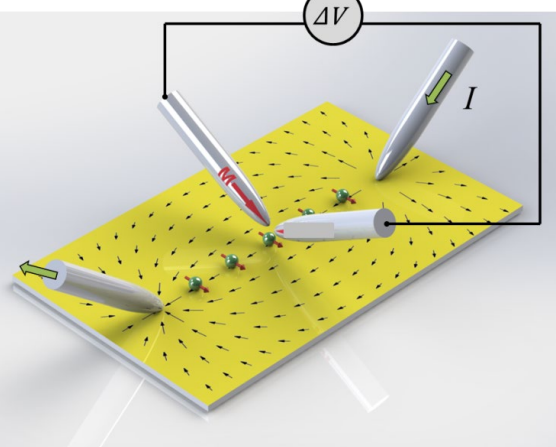
- Spin-dependent transport carried by topological surface states.



Spin-dependent transport in topological insulators

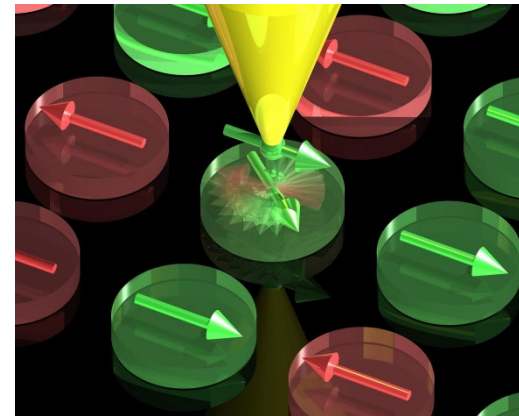
- 4-probe STM transport measurement

Four-Probe STM



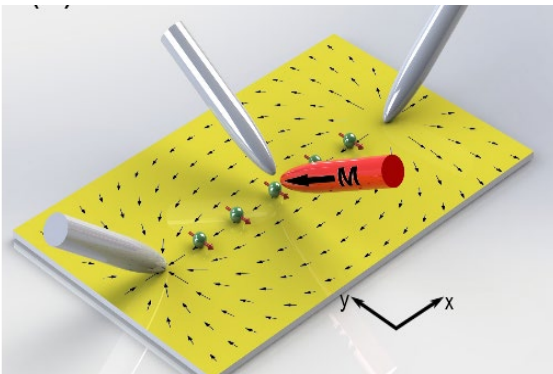
T. H. Kim et al, RSI 78, 123701 (2007)

Spin-Polarized STM



Stefan Krause, Universität Hamburg

Spin-Polarized Four-Probe STM



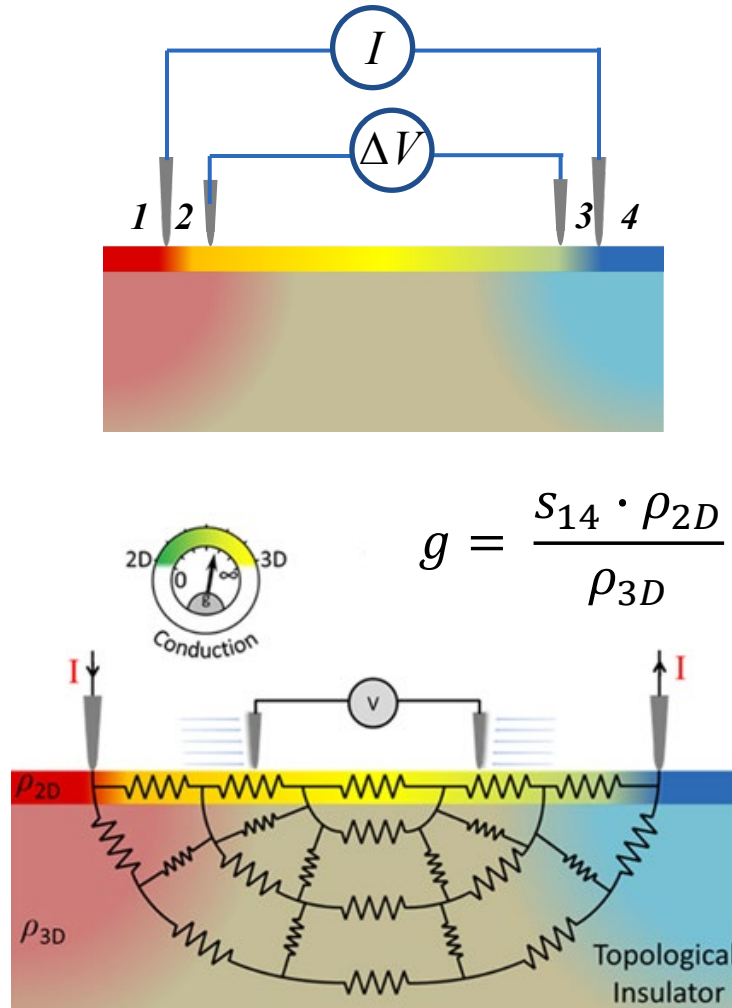
S. M. Hus et al., PRL 119 137202 (2017)

Advantage:

- UHV *in situ* cleaved surface
- Clean and minimal stray field from electrical contacts
- Distinguish and quantify the 2D and 3D conductance
- Differentiate the spin polarized and spin averaged currents

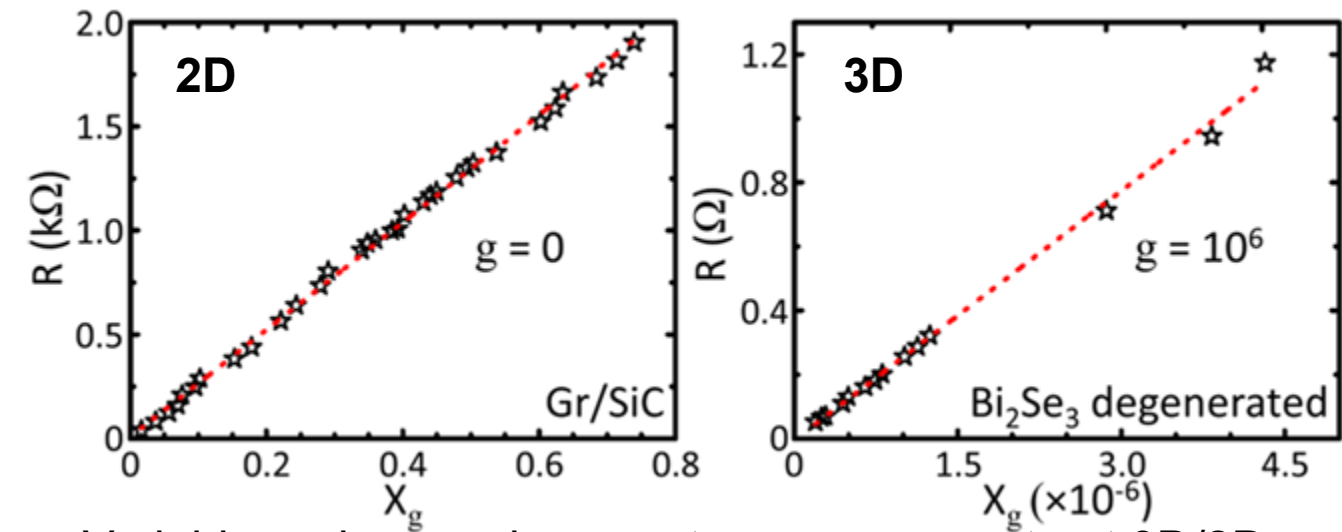
Four-probe STM studies on topological insulators

- Differentiating bulk and surface conduction



$$g = \frac{s_{14} \cdot \rho_{2D}}{\rho_{3D}}$$

$$R = \frac{\Delta V}{I} = \rho_{2D} \cdot \frac{1}{2\pi} \ln \left[\frac{\left(g + \frac{s_{14}}{s_{12}} \right) \left(g + \frac{s_{14}}{s_{34}} \right)}{\left(g + \frac{s_{14}}{s_{13}} \right) \left(g + \frac{s_{14}}{s_{24}} \right)} \right] = \rho_{2D} \cdot X_g$$

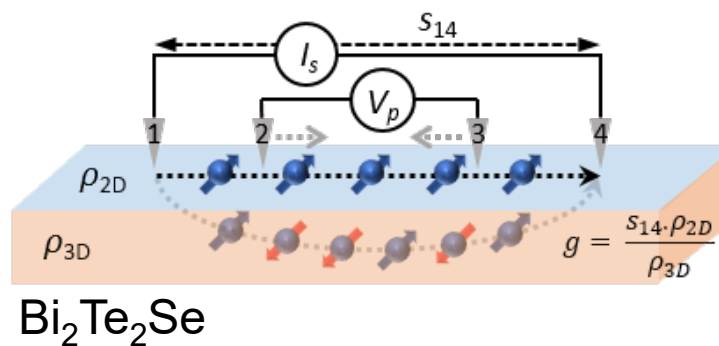


Variable probe-spacing spectroscopy can extract 3D/2D conductivity ratio g

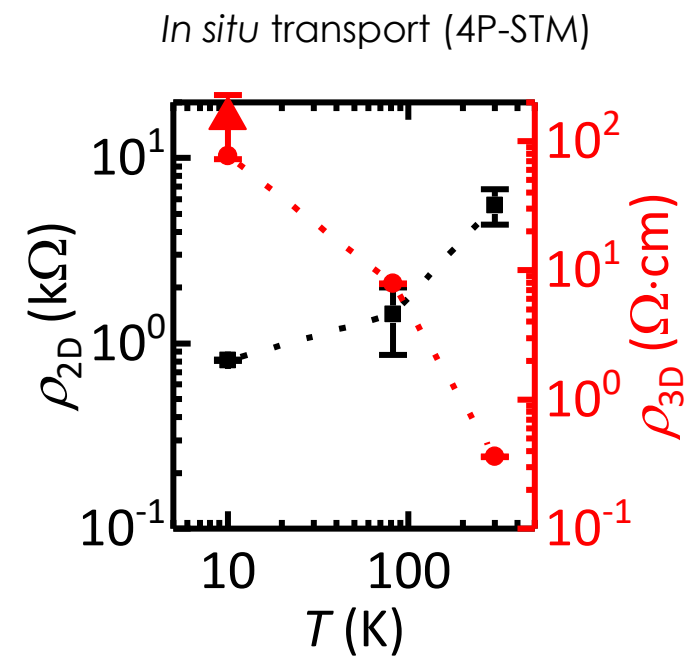
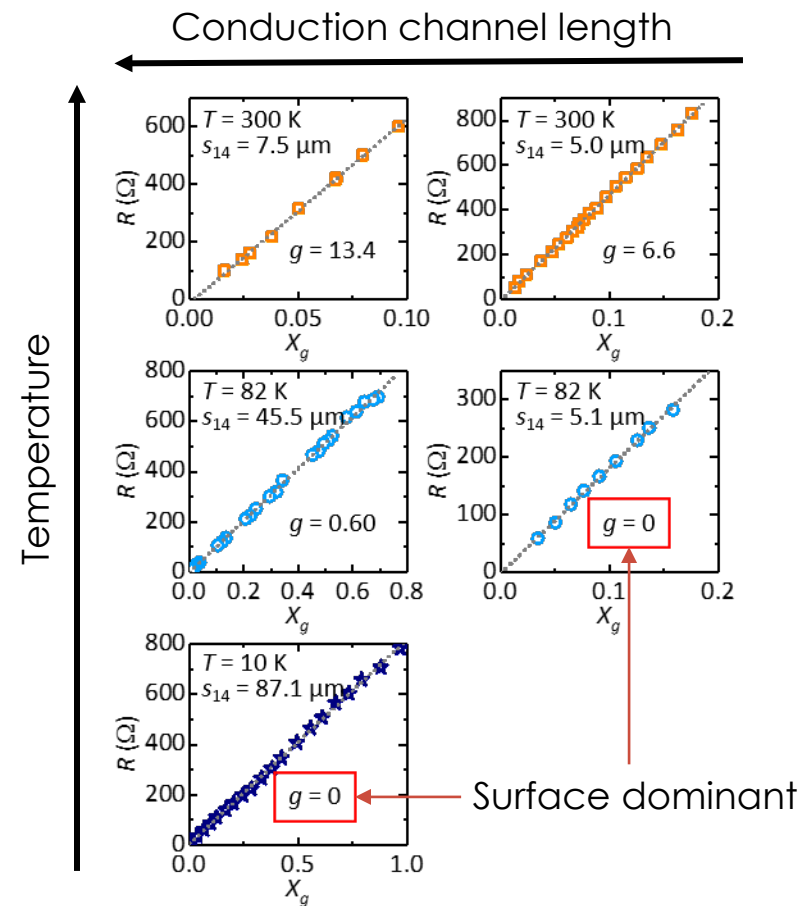
C. Durand *et al.*, *Nano Lett.* **16** 2213 (2016)

Multiprobe STM studies on topological insulators

- Crossover of bulk-surface conduction in $\text{Bi}_2\text{Te}_2\text{Se}$

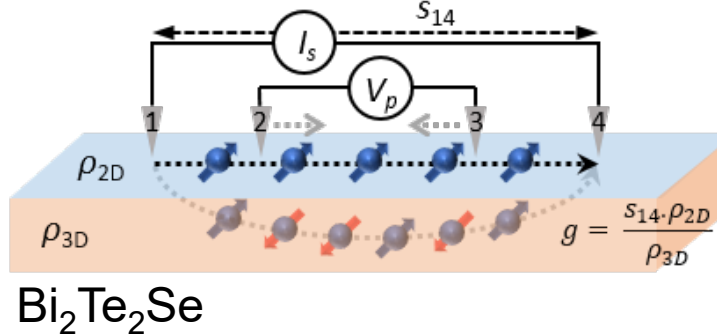


$$g(T, s_{14}) = \frac{s_{14} \cdot \rho_{2D}(T)}{\rho_{3D}(T)}$$



Multiprobe STM studies on topological insulators

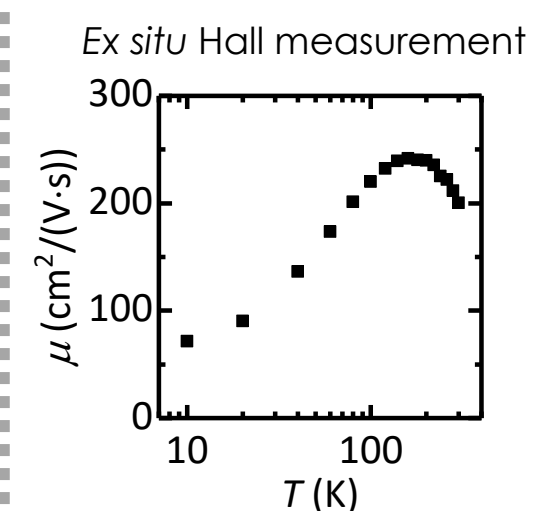
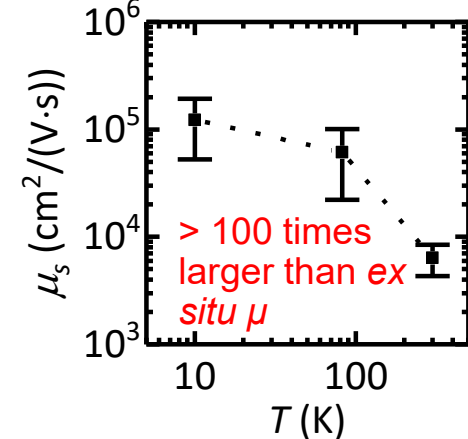
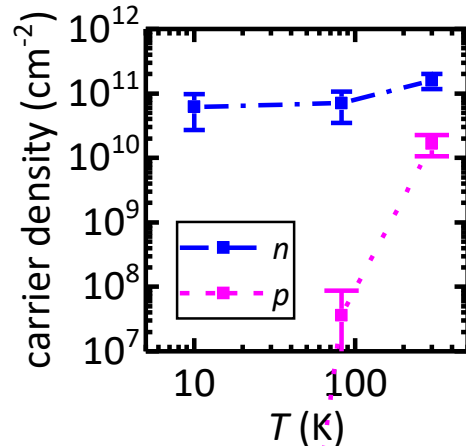
- High surface mobility from topological protection



$$g(T, s_{14}) = \frac{s_{14} \cdot \rho_{2D}(T)}{\rho_{3D}(T)}$$

$$H = \hbar v_F \boldsymbol{\sigma} \cdot \boldsymbol{k} + E_D$$

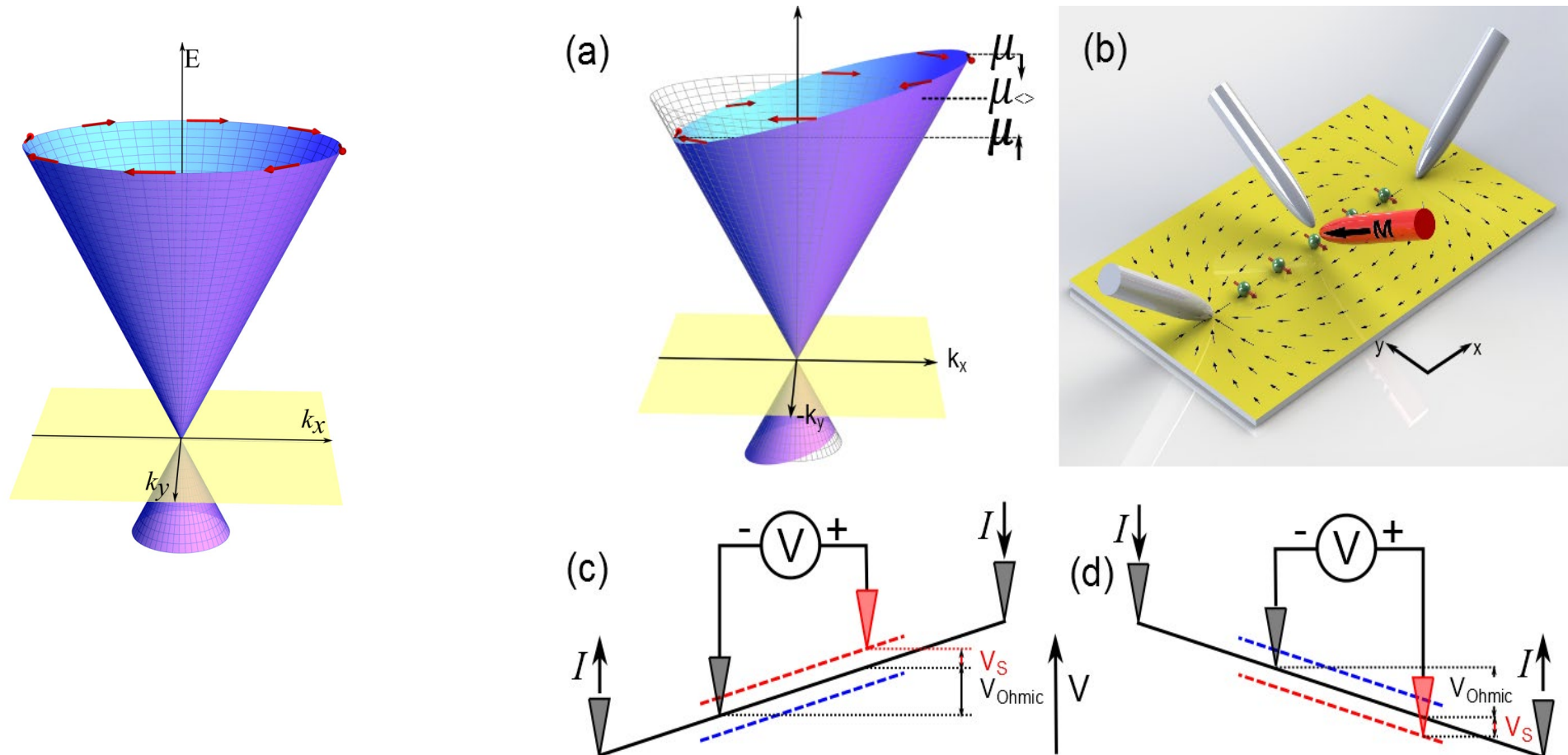
($E_D = -35 \pm 10$ meV, $v_F = (6 \pm 1.5) \times 10^5$ m/s)



W. Ko *et al.*, PRL 121 176801 (2018)

Multiprobe STM Studies on Topological Insulators

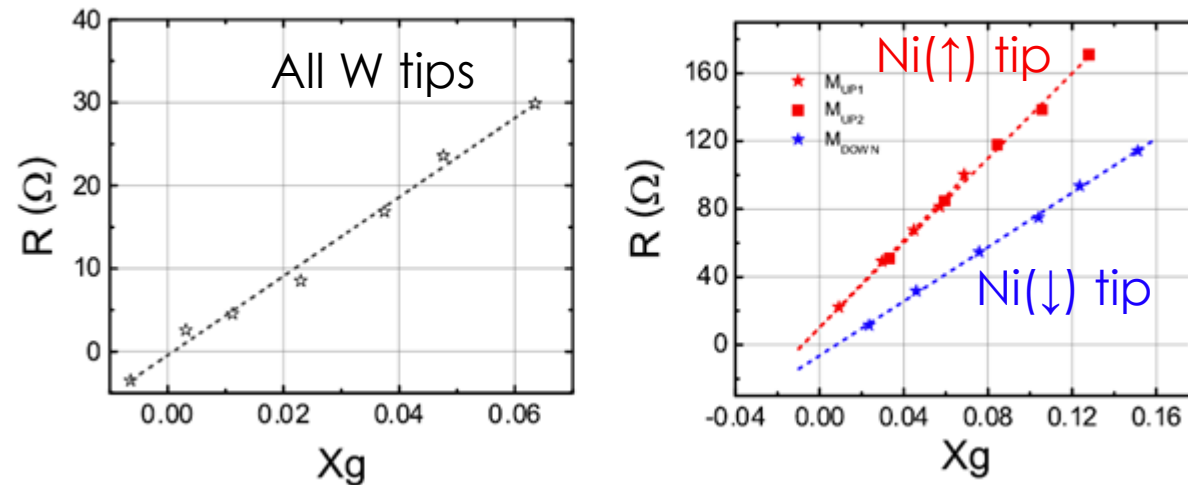
- Spin-dependent transport measurements



Hus, et al., PRL 119, 137202 (2017)

Multiprobe STM Studies on Topological Insulators

- Spin-dependent transport measurements on $\text{Bi}_2\text{Te}_2\text{Se}$

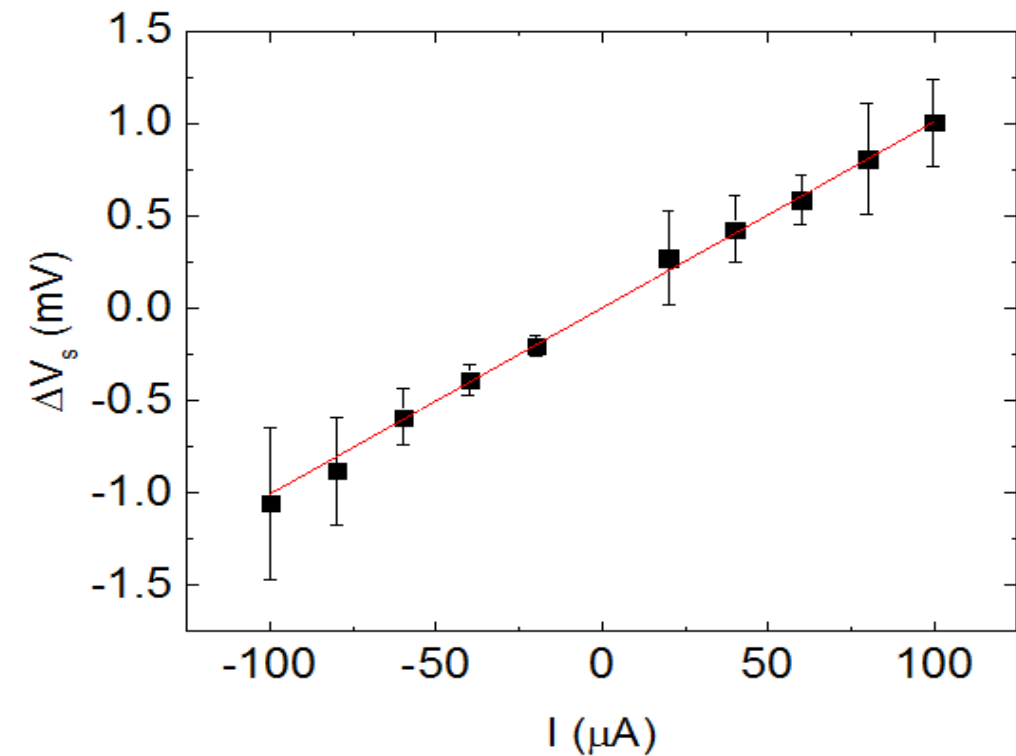
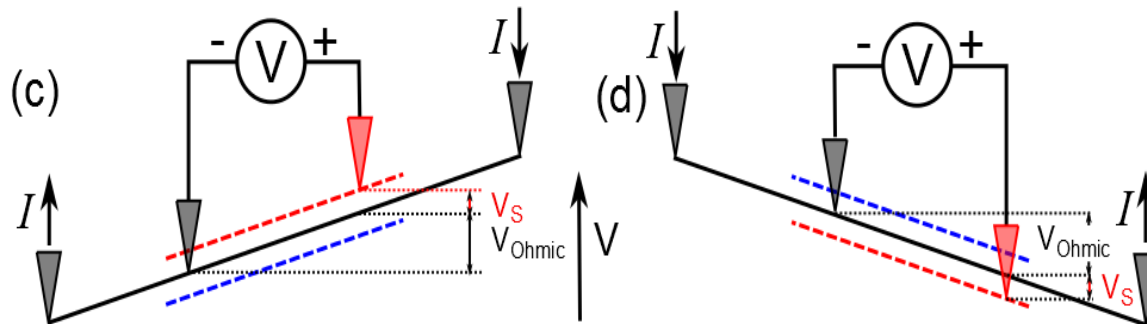


S. M. Hus *et al.*, PRL 119 137202 (2017)

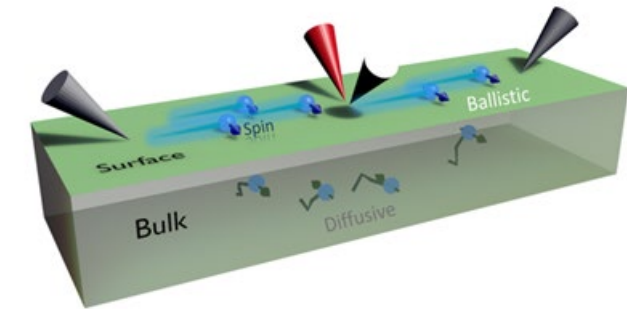
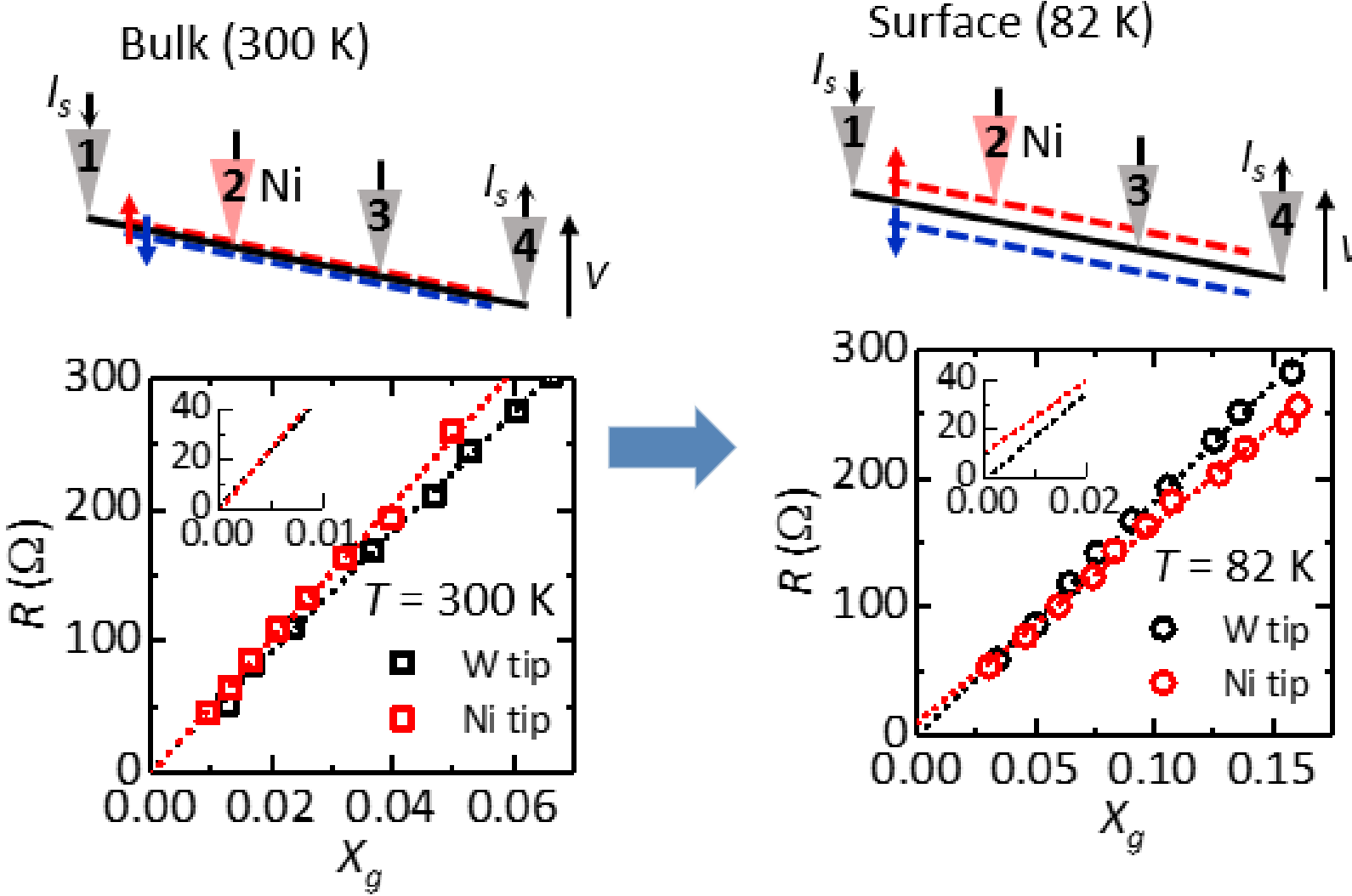
Offset in R at $X_g = 0$ from spin potential

Spin-momentum-locking

- Spin-dependent transport measurements on $\text{Bi}_2\text{Te}_2\text{Se}$



Spin-momentum-locking



Spin polarization $P = 72\%$
comparable to the
theoretical limit for
topological surface states

Mean-free-path $\ell = 1.4 \mu\text{m}$

W. Ko *et al.*, PRL 121 176801 (2018)

Summary

- Scanning tunneling microscopy (STM) allows understanding electronic properties and their relationship with atomic structures.
- Magnetic skyrmions are revealed for the first time in a van der Waals ferromagnet Fe_3GeTe_2 with Spin-polarized-STM
- Current-induced spin polarization and spin-momentum-locked conductance are detected with the first spin-polarized 4-probe-STM